PALEOCLIMATIC VARIATION AND WEATHERING TREND DURING PLEISTOCENE IN THE PESHAWAR BASIN, PAKISTAN

By:

Asad Ali

M.Phil Geology 2020-2022

DEPARTMENT OF EARTH SCIENCES

QUAID-I-AZAM UNIVERSITY ISLAMABAD, PAKISTAN

Acknowledgement

All thanks to Allah, the Most Gracious and Merciful Alhamdulillah, for the strengths and His blessing in completing this thesis. I offer my heartfelt gratitude and admiration to my supervisor, Assistant Professor Dr. Shahid Iqbal, Department of Earth Science at Quaid-I-Azam University Islamabad, who has been a fantastic mentor to me. I'd like to thank you for supporting my research, and your guidance on both research and my career has been invaluable. Sincere gratitude to all my pals, especially Sikandar Shah, Usman Pir Zada, Hasan Raza, and others, for their generosity and moral support throughout my studies. Thank you for the memories and friendship. Finally, my deepest gratitude goes to my beloved parents and my sisters for their endless love, prayers, and encouragement. To those who indirectly contributed to this research, your kindness means a lot to me. Thank you very much.

Asad Ali

(M. Phil Geology)

Abstract

The present study is an attempt to grasp the paleoclimatic variation and weathering trend in the Peshawar Basin during the Plio-Pleistocene epoch. In the northwest, Pakistan the Plio-Pleistocene siliciclastic of the Peshawar Basin provide a geological record of paleoclimatic variations and weathering trend during this time. The sequence indicates basin formation in response to the Attock-Cherat uplifting and preserves paleoclimatic indications during sedimentation. The sedimentary archives are represented in the Peshawar Basin, Pakistan, by an interbedded sequence of mostly sand, silt, and clay rhythmites with interbedded conglomerate and overlain by continuous loess. Sedimentological data suggests that glaciofluvial rhythmites make up the lower portion of the stratal package, which is then covered by floodplain clay cycles, loess deposits, and lastly recent floodplain clays. Petrographic study show that sediments were produced from the recycled orogenic belt under relatively mild weathering conditions, allowing feldspars and other heavy minerals to be preserved. The Chemical Index of Alteration (CIA) is a chemical proxy widely used to determine the degree of source area weathering, while the CIA average values of sand-silt-clay is 59.2 and the loess deposits having values of 50.23. The geochemical proxies show an overall cold arid climate with relatively low chemical weathering. The Rb/Sr ratios in the examined samples range from 0.20 to 0.93 (average: 0.53), while the Th/U ratio average is 5, which is above from the standard value (3.5 to 4.0), so it indicates low to modest degree of chemical weathering at the sediment source. The CIA and PIA values indicate primarily low to modest weather conditions. The chemical weathering history suggests that the Plio-Pleistocene epoch experienced a cool, arid, and humid climate.

Table of Contents

Chapter 1 Introduction **1**

1.1 Introduction 1

1.2 Hypothesis and research questions 2

1.3 Location and accessibility 2

1.4 Climate 3

1.5 Objective 4

1.6 Methodology 4

1.6.1 Field work 4

1.6.2 Petrography 5

1.6.3 Geochemistry 5

1.7Previous work 5

Chapter 2 GENERAL GEOLOGY **7**

2.1 Regional Tectonics 7

2.2 Geological Settings of the study area 8

2.3General Stratigraphy of Peshawar basin. 10

2.4 Stratigraphy of the study sections 10

2.4.1 Faizullah Garhi Section 11

2.4.2 Mandanni Khwar Section 12

2.4.3 Nowshera South section 12

Chapter 3 RESULTS **14**

3.1 Outcrop data/Field work 14

3.1.1 Mandanni Khwar section 14

3.1.2 Faizullah Garhi section 14

3.1.3 Nowshera South section 15

3.2 Petrographic studies 17

3.2.1Quartz. 17

3.2.2 Feldspars. 18

3.2.3 Lithic fragments 18

3.3 Point counting 19

3.4 Geochemical analyses 21

3.4.1 Chemical index of alteration (CIA) 23

3.4.2 Plagioclase Index of Alteration (PIA) 24

3.4.3 Al_2O_3 vs. CIA plot 25

3.4.4 K_2O/Na_2O versus CIA plot 26

3.4.5 A–CN–K plot 26

3.4. 6 Chemical maturity proxy plot 27

Chapter 4 INTERPRETATION AND DISCUSSION **29**
Introduction 29
4.1Sedimentology and lithofacies correlations 29
4.1.1 Conglomerate lithofacies/Alluvial Fan lithofacies 29
4.1.2 Interbedded claystone and siltstone lithofacies/Floodplain clay lithofacies 30
4.1.3 Interbedded sand and silt lithofacies/Lacustrine-Fluvial lithofacies 31
4.1.4 Loess lithofacies 32
4.2 Lithofacies associations 32
4.2.1 Floodplain Clay Lithofacies Association (FCLA) 33
4.2.2 Lacustrine Fluvial Lithofacies Association (LFLA) 33
4.2.3 Loess Lithofacies Association (LLA) 33
4.3 Petrographic studies 34
4.4 Geochemical analysis 36
4.4.1 Chemical index of alteration 36
4.4.2 Al_2O_3 vs. CIA plot 36
4.4.3 K_2O/Na_2O versus CIA plot 37
4.4.4A-CN-K Plot 38
4.4.5 Chemical maturity proxy plot 39
4.4.6 Paleoclimate interpretation 39
4.4.7 Weathering trend 40
SUMMARY AND CONCLUSION **41**
SUMMARY **41**
CONCLUSION **43**
REFRENCES **45**

LIST OF FIGURES

Figure 1.1	Locations of the studied sections on a The Peshawar basin's geological map. Numbers used in map for different studied sections (Modified from the Geological Survey of Pakistan 1993).	3
Figure 2.1	(a) Geographic position of Pakistan. (b) Tectonic map of northern parts of Pakistan showing Peshawar basin. (c) tectonic map of Peshawar basin and study sections (Modified after Bibi et al, 2019).	9
Figure 2.2	Peshawar Basin generalized stratigraphy and comprehensive Pleistocene stratigraphy, including dated periods and major tectonic events (Bibi et al., 2019).	10
Figure 2.3	Lithological logs of the measured stratigraphic sections in the Peshawar Basin.	12
Figure 3.1	Outcrop view of Faizullah Garhi section.	15
Figure 3.2.	Overview of bentonite-rich clay of Mandanni Khwar section	16
Figure 3.3	Channel bed cutting into strata in Faizullah Garhi section	16
Figure 3.4.	The lower part of Nowshera South section having poorly sorted conglomerate	17
Figure 3.5.	Photomicrograph of representative thin sections, (a). It represents Nowshera south 1 thin section, having slate clasts and plutonic Quartz. (b). K-feldspar and plutonic quartz present. (c) the arrow is towards plagioclase, while the green colour represents heavy mineral. (d). Mica flakes and plutonic quartz present in this thin section.	18
Figure 3.6.	Photomicrograph showing the point counting procedure.	19
Figure 3.7.	Quartz-Feldspar-Lithic fragments plot for the representative samples. Q = Quartz, F = Feldspar and L=Lithic fragments. (Dickinson and Suczek, 1979).	20

Figure.3.8.	Log–log plot of polycrystalline quartz (Q_p/F + R) vs. total quartz T_{otal}/F + R (Suttner and Dutta, 1986). The five samples from the humid zone suggest that clasts derived from the local mature Palaeozoic sedimentary quartzite.	21
Figure 3.9.	Al_2O_3 % versus Chemical Index of Alteration (CIA) plot for the representative samples (after Goldburg and Humayun, 2010).	26
Figure3.10.	Plot of chemical index of alteration versus K_2O/Na_2O (after Goldburg and Humayun, 2010).	26
Figure 3.11.	A–CN–K plot for the representative samples, positions of reference minerals (muscovite, illite, smectite, and kaolinite) are given. CaO* = Calcium oxide content in the silicate component. (Young, McLennan, and Keays, 1996). The LFLA and LLA occupy close position to the UCC and ACC while the FPLA samples are close to PAAS and NASC. UCC = Upper Continental Crust, ACC = Average Continental Crust, PAAS = Post-Archaean Australian Shales, NASC = North American Shale Composite.	27
Figure 3.12.	Chemical maturity proxy plot for SiO_2 versus Al_2O_3+K_2O+Na_2O (Malick and Ishiga, 2016; Suttner and Dutta, 1986). showing paleoclimatic conditions during the deposition.	28
Figure 4.1.	Alluvial fan lithofacies and lacustrine fluvial lithofacies at Nowshera south section.	30
Figure 4.2.	Interbedded claystone and siltstone lithofacies of Mandanni Khwar section.	31
Figure 4.3	Alluvial fan lithofacies, Loess lithofacies and Lacustrine-Fluvial lithofacies at Mandanni khwar section.	32
Figure 4.4	Quartz-Feldspar-Lithic fragments plot for the representative samples. Q = Quartz, F = Feldspar and L = Lithic fragments (Dickinson and Suczek, 1979).	35

Figure.4.5.	Log/log plot of polycrystalline quartz (Q_p/F + R) vs. total quartz Q_{total}/F + R (Suttner and Dutta, 1986). The five samples from the humid zone suggest that clasts derived from the local mature Palaeozoic sedimentary quartzite	35
Figure 4.6	Al_2O_3 % versus Chemical Index of Alteration (CIA) plot for the representative samples (after Goldburg and Humayun, 2010). FPLA = Floodplain lacustrine lithofacies association, LFLA = Lacustrine-Fluvial lithofacies associations and LLA = Loess lithofacies associations.	37
Figure 4.7.	Plot of chemical index of alteration versus K_2O/Na_2O (after Goldburg and Humayun, 2010).	37
Figure 4.8.	A–CN–K plot for the representative samples, positions of reference minerals (muscovite, Illite, smectite, and kaolinite) are given. CaO* = Calcium oxide content in the silicate component. (Young et al., 1996). UCC = Upper Continental Crust, ACC = Average Continental Crust, PAAS = Post-Archaean Australian Shales, NASC = North American Shale Composite	38
Figure 4.9.	Chemical maturity proxy plot for SiO_2 versus $Al_2O_3+K_2O+Na_2O$ (Malick and Ishiga, 2016; Suttner and Dutta, 1986). showing paleoclimatic conditions during the deposition.	39
Figure 4.10.	Th(ppm) vs Th/U plots (McLennan, 1993) indicates low degree of weathering of studied sections.	41

LIST OF TABLES

Table 1.0.	Table of latitude and longitude of study sections.	2
Table 3.1.	Framework mineralogical Composition of selected samples.	21
Table 3.2.	Major oxides percentage in Mandanni Khwar, Faizullah Garhi proper and Nowshera South sections.	23
Table 3.3.	The proportions of trace elements and L.O.I of the studied samples.	24
Table 3.4.	Chemical Index of Alteration (CIA) values table for study sections.	25
Table 3.5.	Plagioclase Index of Alteration (PIA) values table of studied sections.	26
Table 4.1	Summary, field features, lithofacies and lithofacies associations of studied sections.	34

CHAPTER 1

INTRODUCTION

1.1 Introduction

Climatic variation is a continuous process, which brings change in the present environment. Geological records bid direct evidence of past environmental change. The globe come across with different climatic events. Pleistocene was the age of tectonic and climatic change in Peshawar Basin. The disturbance in Peshawar Basin due to climate and tectonic activity during Pleistocene age cause the Pleistocene global climate trends resulted in significant regional climate event, which are recorded in sedimentary sequences (Abramowski et al., 2006; Chevalier et al., 2011; Menounos et al., 2013; Stübner et al., 2017; Ehlers et al., 2018). The Pleistocene global climatic variation in the Himalaya is recorded 1–10 ka Indian Summer Monsoon (ISM) cycles and 40–100 ka glacial–interglacial cycles (Singh et al., 2001; Owen et al., 2002; Goodbred, 2003). As a result of this event fluvial discharge in various rivers and river basins which create a link between the fluctuation and the landscape. In the Indus drainage system, more than 36 catastrophic floods have been documented over the last 200 years, such flood resulted change in sedimentation as well as deposition pattern of the sediments. Deposition pattern in Peshawar basin represents the variation in past climate. Generally, the deposition in Peshawar Basin is Stacked sequences of fining-upward sediments. Present study is an attempt to know the climatic variations and weathering trend in Peshawar Basin.

1.2 Hypothesis and research questions

Major part of the Peshawar Basin is covered by Pliocene to Pleistocene sediments in a generally stacked sequences of fining-upward sediments. The sediments are mainly clay, sand, and gravel. The uplifting of the Attock–Cherat ranges during the Middle to Late Pleistocene repeatedly blocked

the outflow of the Indus and Kabul rivers and produced large lakes within the Peshawar Basin. The conglomerates and gravels indicate the periodic catastrophic floods conditions. There are different questions rise about the preserved sequence of Pliocene to Pleistocene sediments like:

1. What was the deposition style during the Plio-Pleistocene in the area?
2. What was the paleoclimatic variation and weathering trend during the Plio-Pleistocene?

1.3 Location and accessibility

The Peshawar Basin lies 150 km north of the active front of Himalayan deformation at the Salt Range and 50 km south of the Main Mantle thrust. The study area situated between latitude 33^0 51′ 88″ N to 34^0 19′ 69″ N and longitude 71^0 42′ 706″ E and 71^0 54′ 436″ E. Study sections located in the Nowshera district of the Khyber Pakhtunkhwa. The southern study section is located near to Kabul River in south of Nowshera. All study sections are easily accessible by several metaled and unmetalled roads from Nowshera, Mardan, Charsada, and Peshawar. Nowshera South is 25 km away from the Mardan city and 8 km from Nowshera city. Table of latitude and longitude of study sections is given below.

Table 1.1 Table of latitude and longitude of study sections.

Location	Latitude	Longitude	Position
Mandanni Khwar	33^0 51′ 88″ N	71^0 42′ 706″ E	Starting
Faizullah Garhi	33^0 50′ 28″ N	71^0 41′ 98″ E	Starting
Nowshera South	34^0 00′ 05″ N	71^0 58′ 07″ E	Starting

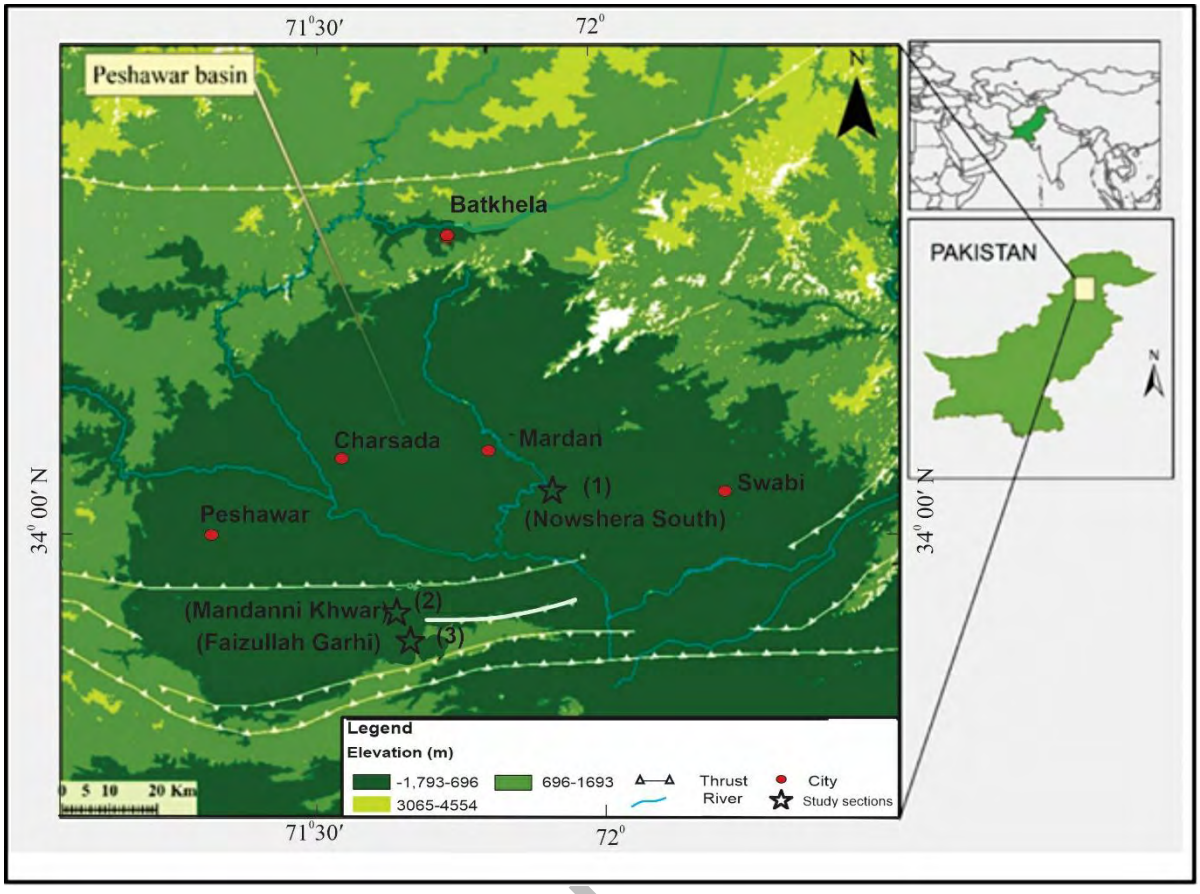

Figure 1.1. Locations of the studied sections on a The Peshawar basin's geological map. (Modified from the Geological Survey of Pakistan 1993).

1.4 Climate

The study sections are in sub-tropical low relief land. The elevation of study section is 432 m. Temperature in summer is too hot in Nowshera, Faizullah Garhi and Jalala, while moderate in winter season. The maximum temperature reach in summer season up to *43*°C and low 27 °C. The duration of summer is 5 months from May to September. While the duration of winter in study sections is 3 months start from December to February. The average temperature in winter season in study sections are 24°C. The average annual precipitation is 400 mm/year, of which 200 mm occurs in the winters (Pak Met, 2015). The favourable weather for field is winter specially February. The hottest month of the year in study section is June. The Monsoon starts in July and cause heavy rainfall in such area which cause flood in local drainage system.

1.5 Objective

The main objective of the present study is an attempt to investigate the following.

1. To find out the climatic fluctuations and weathering trend in Plio–Pleistocene of the Peshawar Basin.
2. Revision of the present stratigraphic framework for the Plio–Pleistocene of the Peshawar Basin Pakistan based on field observation, petrography, and bulk geochemistry.

1.6 Methodology

To find out the climatic variation and weathering trend in Plio–Pleistocene stratigraphic succession within the Peshawar Basin detailed sampling from different sections are taking which cover all the variations in facies. Rocks samples were collected for sediment petrography and geochemistry. The three different sections were sampled. The sampling was based on lateral and vertical variations. The sections beds are measured, and different sedimentological features are recorded. The sample were studied further petrographically also find out geochemical analysis through different laboratory procedures. The description of methods, which are used for present work are following.

1.6.1 Field work

The Plio–Pleistocene stratigraphic succession within the Peshawar Basin was sampled at three different sections (Mandnni Khwar, Faizullah Garhi, Nowshera South sections). All the sections having clay, silt, sand, and conglomerate. Samples were collected after some variation or presence of any sedimentological features. 23 samples were collected from sections for geochemistry, while 15 samples were selected for thin sections and petrographic studied because of presence of conglomerates and gravels.

1.6.2 Petrography

Thin sections of selected samples were prepared in Earth Sciences Department, Quaid-i-Azam University, National Centre of Excellence in Geology Peshawar and studied under Leica DM2700P microscope present in petrography Lab at Earth Sciences Department Quaid-i-Azam University, Islamabad. Several types of grains are analysed through Image J software installed in Lab computer systems.

1.6.3 Geochemistry

Based on field data 23 samples were selected for geochemical analyses The chemicals analysed included oxides, major, minor, trace, and rare earth elements (REE). For the extraction of Si, Nb, and Rb, each sample 0.2 mg split was fused in lithium metaborate/tetraborate and digested in nitric acid.

1.7 Previous Work

The first study of southern portion of the Peshawar Basin was given by Coulson in 1938, who included these rocks in Attock Slate and assigned Precambrian age to this sequence. Reef complex of Silurian and Devonian age in Nowshera discovered by Teichert and Stauffer (1965). Ali and Anwar (1969) described the stratigraphy of Nowshera Reef Complex. Latif (1970) collects corals from Nowshera Formation and assigned Carboniferous age. Fuchs (1975) tried to explain the Palaeozoic succession of Peshawar Basin in the Himalayan stratigraphic framework. He also explains the stratigraphy of several bedrock inliers near Swabi and Nowshera. Molloy (1979) described the most detailed bio stratigraphic information of Peshawar Basin.

The basin filling sediments detailed analysis attempted by different researcher in different years, (Cotter, 1933; Latif, 1970; Tahirkheli, 1970; Calkins, 1974; Meissner, 1974) Burbank and Tahirkheli (1985) designated the Pliocene to Pleistocene sequences and describe its thickness ranges up to 300 m, which are generated by the sedimentation rate ranging between 2cm/1000 to

15/1000 years. Bibi et al. (2019b) highlighted the source to sink relationship of Plio-Pleistocene sedimentary sequence present in Peshawar Basin.

CHAPTER 2

GENERAL GEOLOGY

This chapter describes the study area's general geology, including tectonics, structural geology, and stratigraphy. The regional tectonic setting of Pakistan, as well as the tectonic framework of study sections, are covered in detail. A structural and tectonic map of the study area is also included. The stratigraphic framework of the Peshawar Basin, as well as a stratigraphic chart, are also included in this chapter.

2.1 Regional Tectonics

Pakistan comprises of Indo-Pakistan, Arabian and Eurasian Plates. It has a vital role in forming structures like fold thrust belt and huge mountains. Some of the plates are still active like Arabian Plate subducted beneath the Eurasian Plate. The Indian Plate separated from the Gondwana Continent around 120 Ma, drifted northward about >4000 km, and collided with the Eurasian Plate in the Paleogene with the closure of the Tethys (Molnar and Tapponnier 1975; Klootwijk et al., 1992; Petterson and Treloar 2004). The closure of Tethys causes an island arc called Kohistan Island Arc, this island as sandwiched between Eurasian and Indo-Pakistan Plates marked by two suture zones, i.e., Indus Tasngpo Suture Zone (in South) and Shyoke Suture Zone (in North) (Kazmi & Jan, 1997). The Himalayan orogeny in Pakistan is divided into northern orogeny and western orogeny due to the drifting of Indo-Pakistan Plate and its collision with Eurasian Plate. In northern orogeny convergence occur along leading edge of Indo-Pakistan Plate. The structurally and geometrically complex thin and thin skin deformation of Pakistan have resulted from collision along an oblique margin as well as leading edge of Indo-Pakistan and Eurasian Plates (Bender and Raza,1995).

The collision of the Indian and Eurasian Plates caused crustal shortening and lithosphere thickening (uplifting) within the orogen, providing a long-term supply of erosional sediment flux

over time (Clift et al., 2008; DeCelles et al., 2001). The huge mass of the orogen in the north caused the Himalayan deformation front to migrate southward, resulting in the creation of many significant south verging thrust systems (Gansser, 1964; Yin and Harrison, 2000). These thrusts acted as trapping barriers for sediment flux from the north, resulting in intermontane basins of varying sizes.

2.2 Geological Setting of the Study Area

The study area is in the southern part of the Peshawar Basin. The Peshawar basin is situated between the southern Himalayan and Hindu Kush Ranges. Deformation in the region was caused by ongoing Himalayan tectonic activity, which resulted in sets of north dipping thrusts that built massive intermontane basins along the northern foredeep margin. Peshawar Basin is one of these intermontane Basins. Peshawar Basin formed around 2.8 million years ago because of the upheaval of the Attock-Cherat Ranges (Cornwell,1998). This basin is located to the north of the Main Boundary Thrust (Fig. 2.1) on the hanging wall of the Attock-Cherat Ranges. The existence of fault lines in the alluvial succession shows that the basin was deformed during the Late Quaternary period (Yeats and Hussain, 1987). The Malakand, Swat, and Buner metasediments and granitic intrusions are in the north of the Peshawar Basin, while the Gandghar range is in the east of the basin, and the western section of the Peshawar Basin marks the boundary with the Khyber Ranges. The Attock-Cherat Range uplift and movement on the Main Boundary Thrust are thought to have battered the Peshawar Basin sediments (Burbank , 1983a).

During the Late Pliocene, the basin began to accumulate sediments at rates ranging from around 2 cm/1000 year to 15 cm/1000 year, with accumulations exceeding 300 m in thickness along the southern margin. (Burbank and Tahirkheli, 1985). Sedimentation in the Peshawar Basin was carried out by alluvial fans prograde into the basin from the nearby Attock–Cherat Ranges along the southern margin. The central part of the basin has interbedded lacustrine and alluvial sediments because of ponding of Kabul, Kalpani, and Indus. These rivers cause the present-day drainage

system. Major part of the Peshawar Basin is covered by Pliocene to Pleistocene sediments. The southern basin sequences can be up to 300 m thick (Burbank and Tahirkheli, 1985). The Kabul and Kalpani river caused strong channel incision in distinct parts of the Peshawar Basin, which supply better sections for study.

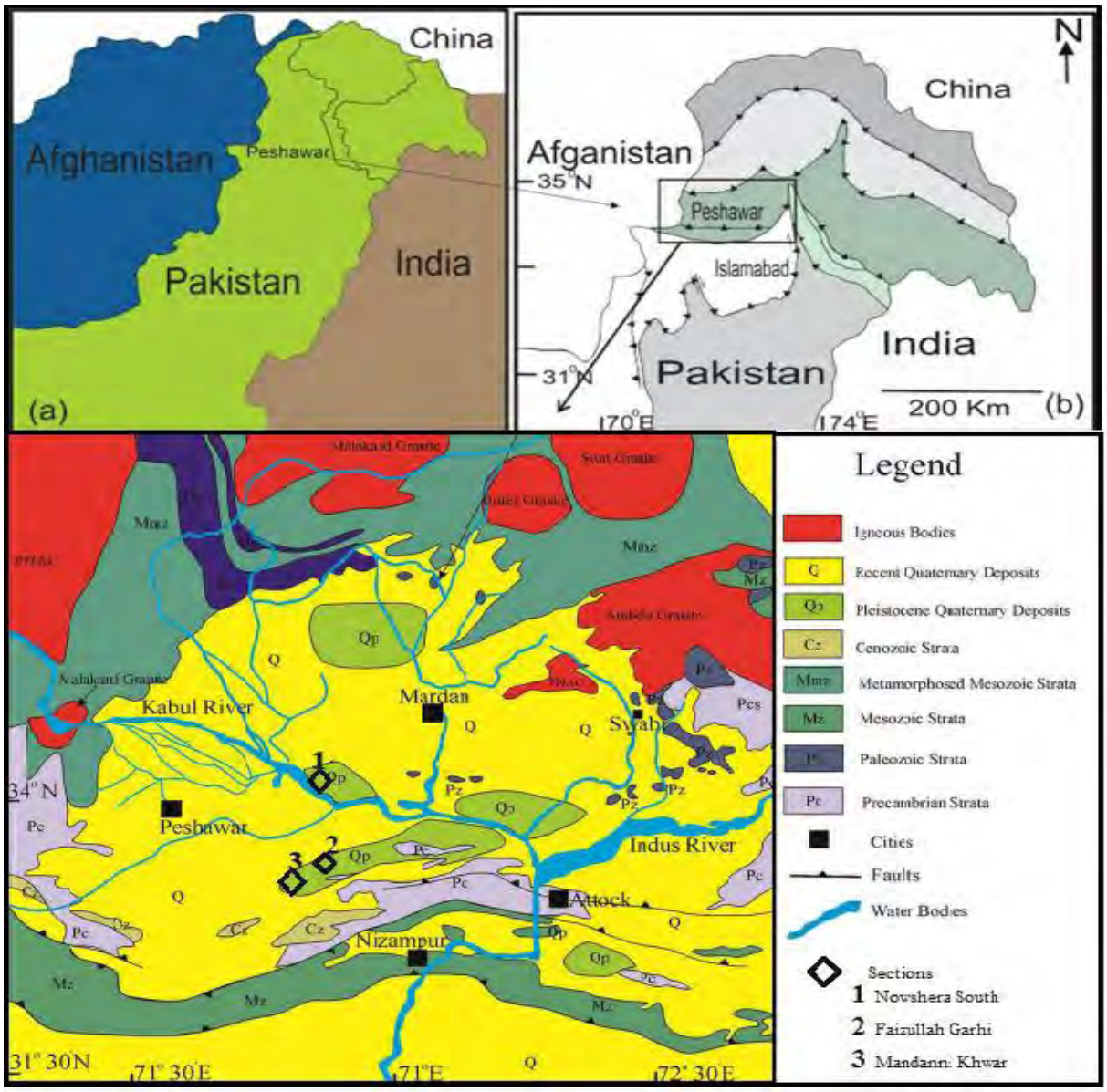

Figure 2.1; (a)Geographic position of Pakistan. (b)Tectonic map of northern parts of Pakistan showing Peshawar Basin. (c) Tectonic map of Peshawar Basin and study sections. (Modified after Bibi et al., 2019).

2.3 General Stratigraphy of Peshawar Basin

Rocks exposed south of the Peshawar Basin, in the Nowshera, Gandghar and Attock-Cherat Ranges, are mostly Precambrian to Devonian metasediment. The oldest Formation in Peshawar Basin are Proterozoic Tanawal Formation, which consists of quartzite and serves as the basement of the basin. The formation is overlain by a complete Palaeozoic succession. (Burbank and Tahirkheli, 1985). The Mesozoic and Lower Cenozoic successions are missing in Peshawar Basin. In the southern part of the basin there is thick succession of lacustrine–floodplain sediments interbedded with fluvial sands and gravel of Plio–Pleistocene age. (Fig. 2.2)

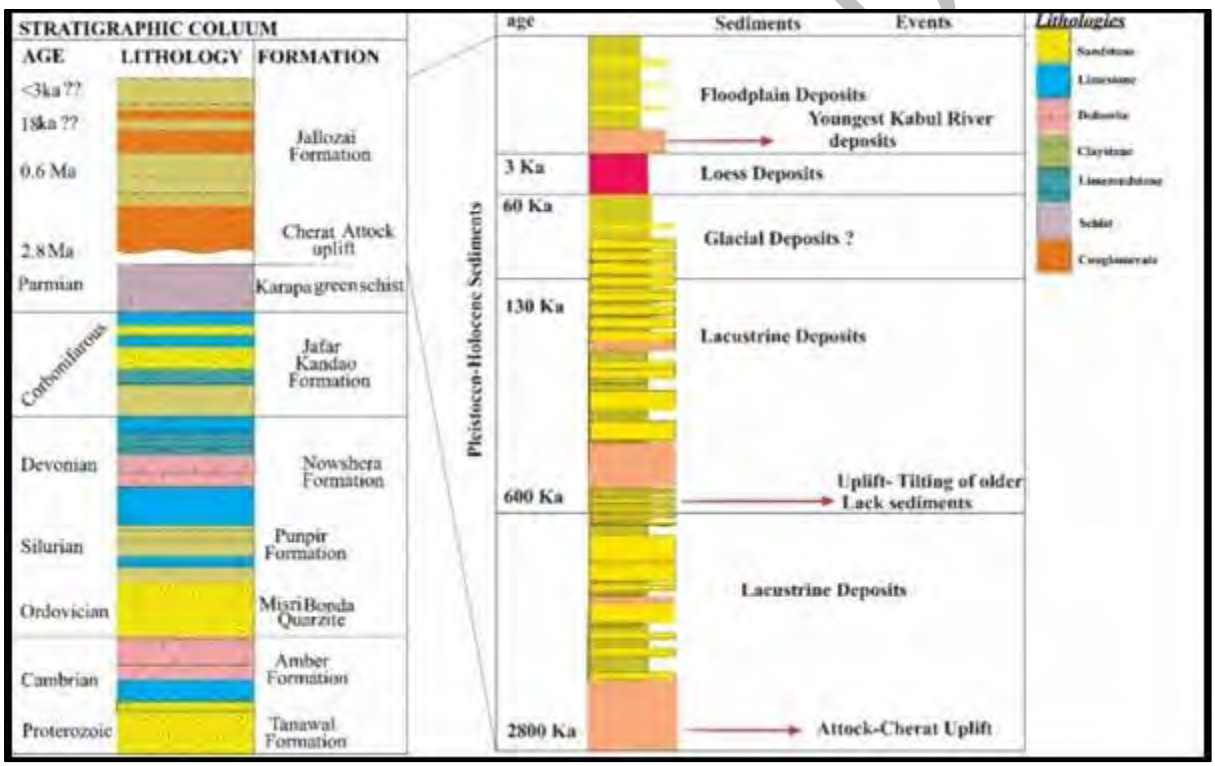

Figure 2.2. Peshawar Basin generalized stratigraphy and comprehensive Pleistocene stratigraphy, including dated periods and major tectonic events (Bibi et al., 2019).

2.4 Stratigraphy of the Study Sections

Peshawar Basin is inclined by the local drainage as an incision, which occur in thick succession of Plio–Pleistocene age. The sedimentation occurs in the form of alluvial fan especially in southern

part of the basin. Natural outcrops of Plio–Pleistocene age sediments are exposed along the banks of these three rivers (Indus, Kabul and Kalpani). The stratigraphy of Plio–Pleistocene age is collectively known as the Jallozai Formation. Lithology of studied sections consists of rhythmic cycle of fine clay, silt, sand, and conglomerate. Detail description of lithology of study sections are following.

2.4.1 Faizullah Garhi Section

This section having little bit variations from Nowshera South section. The section contains conglomerate and several types of clay. i.e., green lamination clay, silty clay, dark clay, and red/pink clay at upper surface. The conglomerates are poorly sorted. There are two layers of conglomerate (Fig. 2.3) in this section. The clasts alignment is common in conglomerate bed, which indicates fluvial environment.

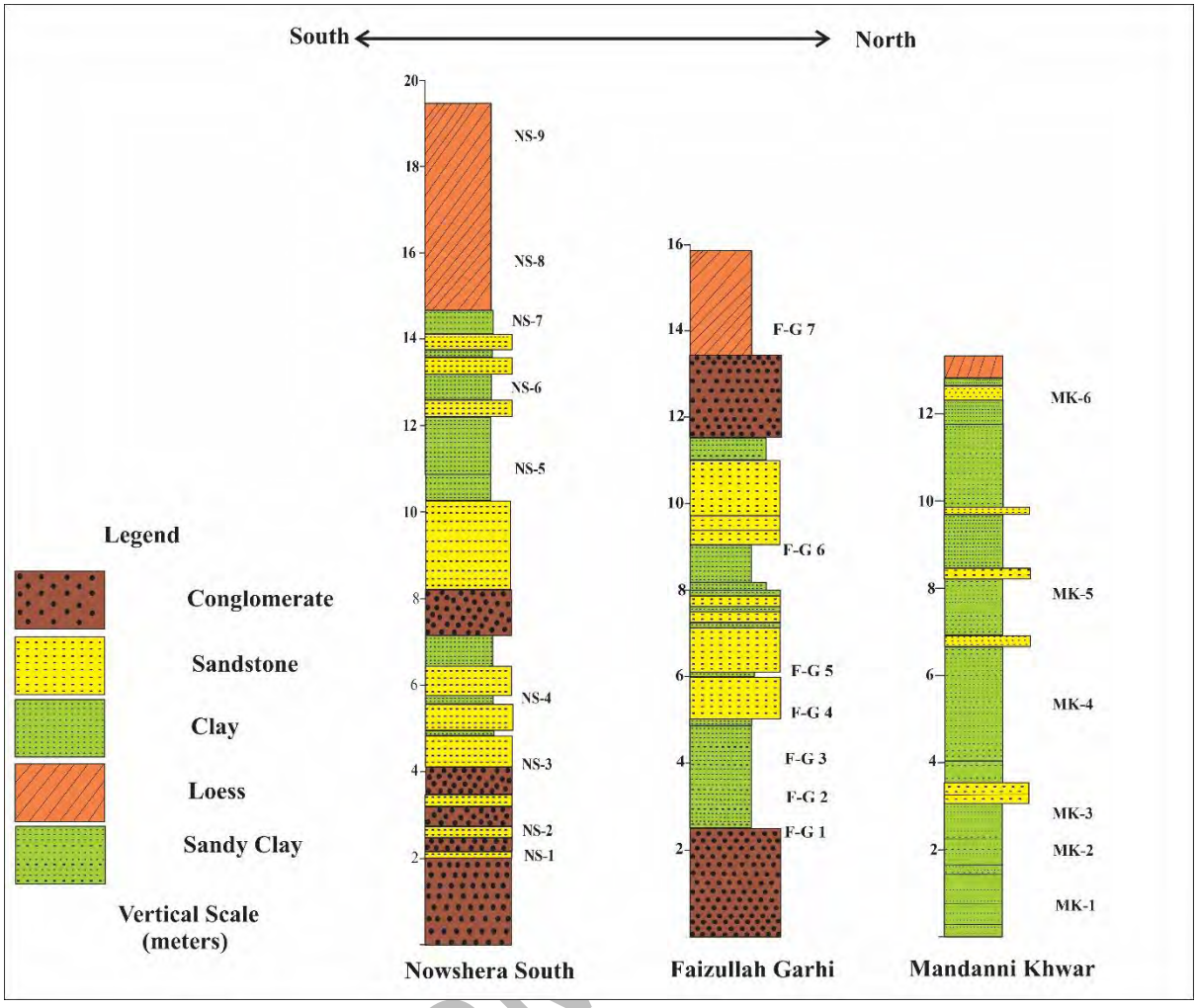

Figure 2.3 Lithological logs of the measured stratigraphic sections in the Peshawar Basin.

2.4.2 Mandanni Khwar Section

In this section the lower part is consist of 30- to 40-cm thick, fining-upward clay rich repeated cycles. Clay of this section is variables in colour as well as in nature. In vertical section the clay colour changes from light grey, greenish grey into dark grey. There are multiple horizons of sandy and silty clay having thin lamination. (Fig. 2.3). The upper part of this section consists of loess deposit which is orange red silty clay.

2.4.3 Nowshera South

Nowshera south section is composed of predominantly alluvial fan sediments. This section consists of clay, silt, sand, and conglomerate. This section contains the multiple layers of poorly sorted

conglomerate. The clast is mainly slate, while limestone and shale also present in small quantity. The clast of conglomerate is aligned parallel to the bedding plane. The lower contact is not expose in this section. On the upper part the loess deposit is present (Fig.2.3).

CHAPTER 3

RESULTS

To understand the paleoclimatic fluctuations and weathering trend in Plio–Pleistocene stratigraphic succession within the Peshawar Basin detailed section measurement and sampling from three sections was conducted which cover lateral and vertical facies variations. The sections beds thickness was measured, and different sedimentological like pinching, mud dykes, fracture and ball pillow structure were recorded. Sampling was conducted for sediment petrography and geochemistry. The description of methods, which have been used for present work and the results are presented in the following lines.

3.1 Outcrop/ field data

There is no proper name in literature for the Plio-Pleistocene strata, while it is known as Jalozai Formation (Tahirkheli, 1970). The Formation formed because of low energy floodplain deposits containing clay and silt zones succeeded by northward-prograding alluvial fans with a source in the Attock-Cherat Ranges (Burbank and Tahirkheli, 1985). Three outcrop sections were observed at Mandanni Khwar, Faizullah Garhi, and Nowshera south have been sampled for further laboratory study. The lithologies of three sections have been correlated with each other. The lithologies of studied sections are given below.

3.1.1 Mandanni Khwar Section

In this section the lower part consists of 30 – 40 cm thick, fining-upward clay rich repeated cycles (Fig. 3.1). Clay of this section is variables in colour as well as in nature. In vertical section the clay colour changes from light grey, greenish grey into dark grey. There are multiple horizons of conglomerates which contain poorly sorted clasts of limestone, sandstone, and shale. The clast of limestone is larger than sandstone and shale clasts. The matrix is sand and clay. The upper part consists of loess deposit which is orange red silty clay.

3.1.2 Faizullah Garhi section

This section displays variations from Mandanni Khwar Section. The section contains conglomerate and different types of clay. i.e., green lamination clay, silty clay, dark clay, and red/pink clay at upper surface. The channel bed cutting into strata and mark a clear contact with orange red silty clay bed (Fig. 3.3). The conglomerates are poorly sorted. Bentonite rich clay also present in this section (Fig. 3.2).

3.1.3 Nowshera South

The Nowshera south section is composed of predominantly alluvial fan sediments. It consists of clay, silt, sand, and conglomerate. This section contains thick layers of poorly sorted conglomerate. The clast is mainly slate, while limestone and shale also present in minor quantity. The clasts of conglomerate are aligned parallel to the bedding planes. The lower contact is not expose in this section. On the upper part the loess deposit is present.

Figure 3.1 Outcrop view of Faizullah Garhi section.

Figure 3.2. Overview of bentonite-rich clay of Faizullah Garhi section.

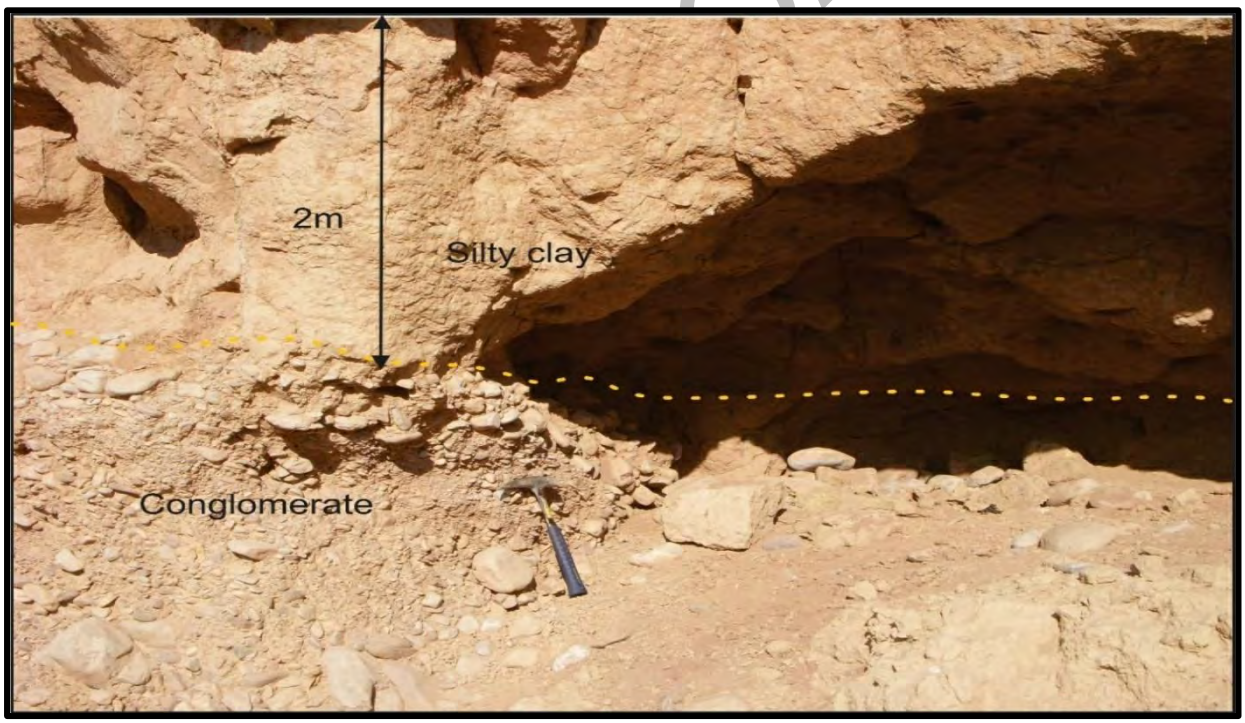

Figure 3.3 Channel bed cutting into strata in Faizullah Garhi section.

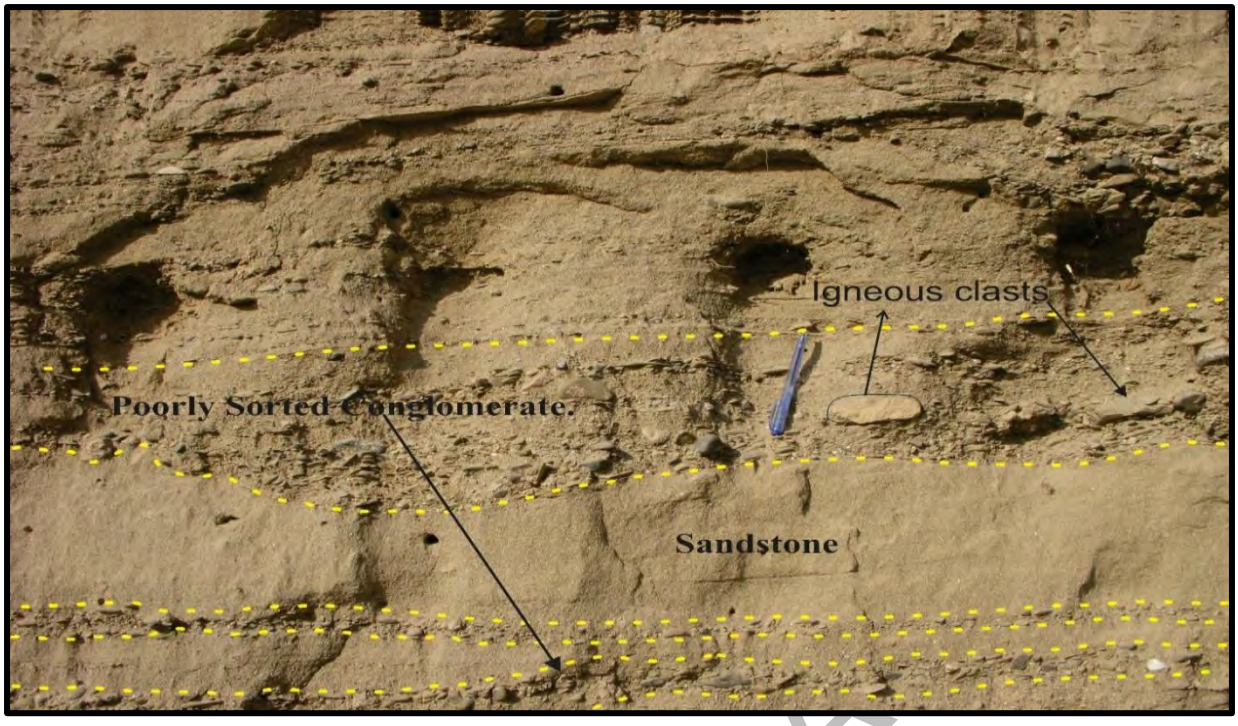

Figure 3.4. The lower part of Nowshera South section having poorly sorted conglomerate.

3.2 Petrographic studies

Thin sections of 15 samples from Mandanni khwar, Faizullah Garhi and Nowshera South sections were studied. All thin sections were studied using Leica DM2700 P microscope with Leica MC170 HD camera in petrographic laboratory Earth Sciences Department Quaid-i-Azam University Islamabad. Modal analysis of thin sections was carried out with the help of Image Analysis software. In thin sections the major constituents are quartz, while small amount of feldspar and lithic fragments are also present. The detail description is given below.

3.2.1 Quartz.

The most common clastic grain is quartz, which comes in monocrystalline (Q_m) and polycrystalline (Q_p) variants. (Table 0-1). The monocrystalline (Q_m) further classified into monocrystalline with unit extinction (Q_{mue}) and undulose extinction (Q_{muu}). The polycrystalline quartz (Q_p) also divided into two categories, Q_p with two-three and $Q_{p>3}$. The monocrystalline quartz grains range from sub-rounded to sub-angular. whereas the polycrystalline quartz grains vary from sub-angular to angular. The grain contacts are straight to suture. Q_{total} contributes for 61.28 percent of the framework's components on average. Q_{mue} is the most common, accounting for 47 % of the total framework composition, followed by Q_{muu} (4%), with Q_{pq} (2–3) content accounting for 3% and $Q_{pq} > 3$ accounting for 7%.

3.2.2 Feldspars.

The feldspars are present in various amounts across the sample areas, two types of feldspars plagioclase and K-feldspars have been identified throughout the samples (Fig3.5). The plagioclase feldspar present in abundant. The average total feldspars (F_t) content of the bulk framework is 5 percent, which is generally fresh and unmodified.

3.2.3 Lithic fragments

The study sections samples contain different types of rocks fragments. Lithic fragments (L_t) make 23 percent of the total in which sedimentary lithics are 2%, while metamorphic lithics are 18% and volcanic lithics are 3%. Heavy mineral (Fig.3.5 d) and mica flakes are present in studied sections. Fig.3.5.

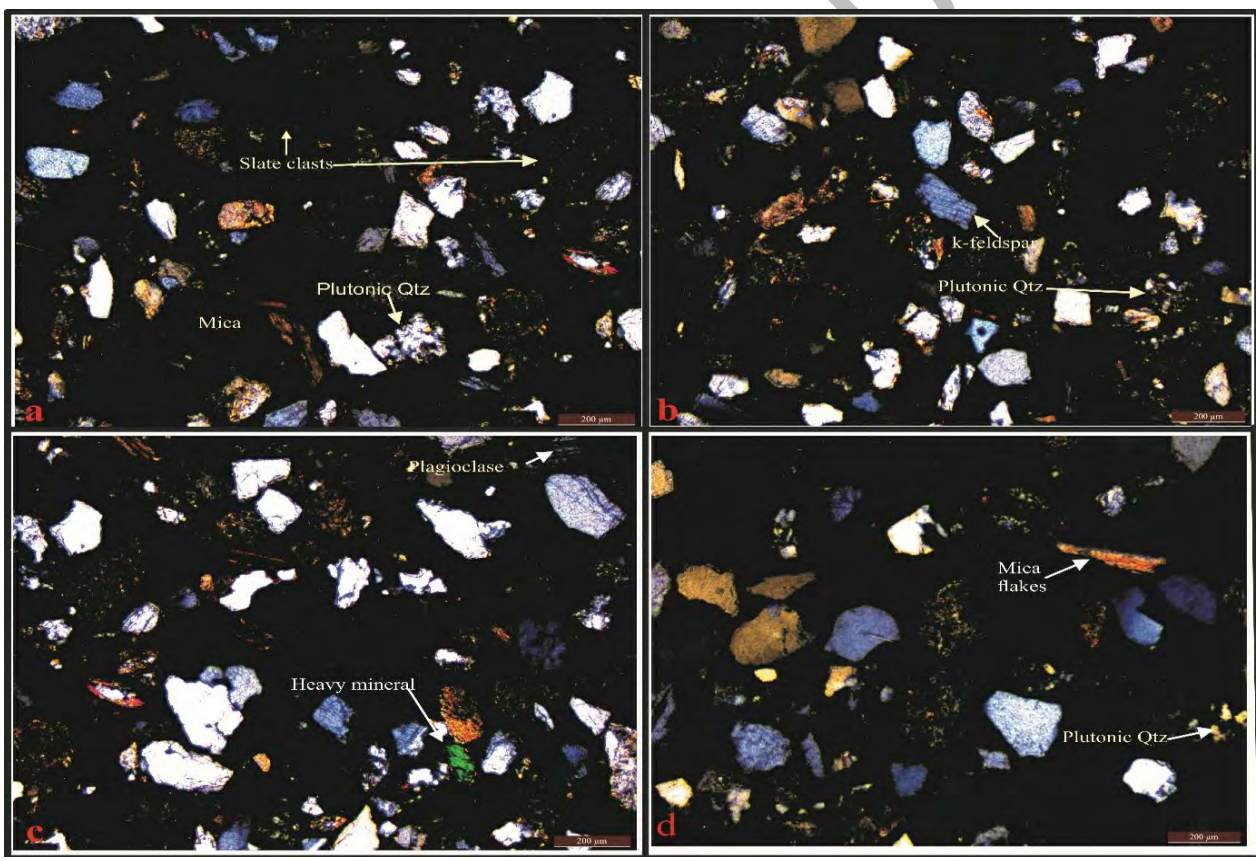

Figure 3.5. Photomicrograph of representative thin sections, (a). It represents Nowshera south 1 thin section, having slate clasts and plutonic Quartz. (b). K-feldspar and plutonic quartz present. (c) the arrow is towards plagioclase, while the green colour represents heavy mineral. (d). Mica flakes and plutonic quartz present in this thin section.

3.3 Point Counting

Dickinson (1970), Graham et al. (1976) and Ingersoll and Suczek (1979) discussed the parameters and methods for identification of framework minerals. The technologically advanced and digital image software Image J was utilized for point counting analysis. Three microphotographs were taken from the bottom, middle, and top of each thin section to gather information about the minerals. The microphotograph was imported to software J and then applied grid to each image (Fig. 3.6). The grid on the centre of grains is counted 1 while on the edge of grain was counted 0.5. total 300 points were counted for each photomicrograph.

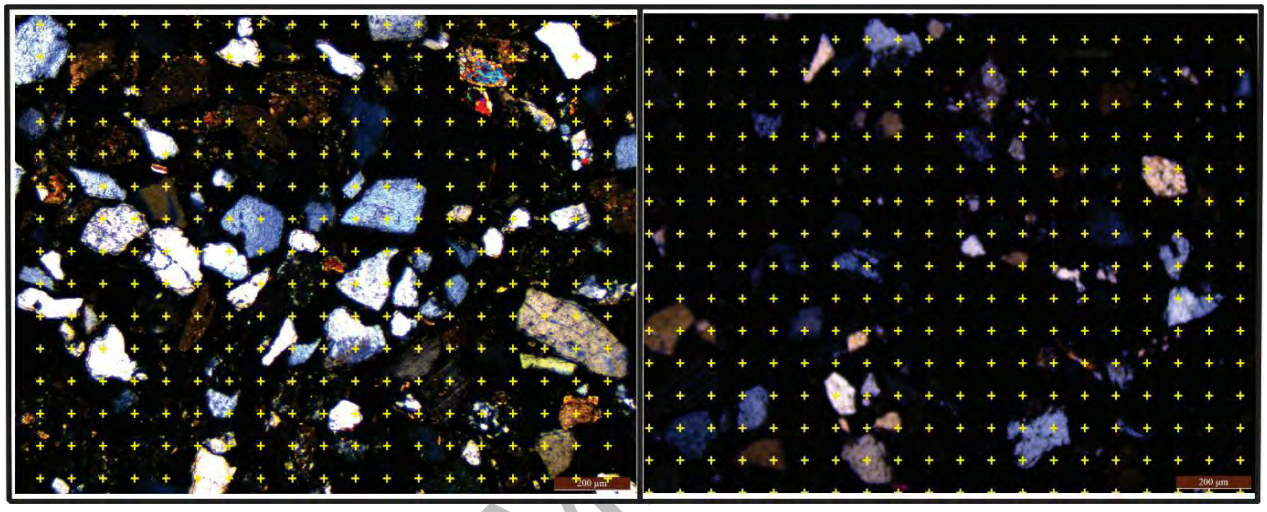

Figure 3.6. photomicrograph showing the point counting procedure.

The lithic fragments are represented with Lv=Volcanic/igneous lithic, L_m =Metamorphic lithic and L_s= Sedimentary lithics (Table .0-1), A= Alkali-Feldspar, P=Plagioclase Feldspar, M= Mica, D=Denser mineral

Table 3.1. Framework mineralogical Composition of selected samples.

S. No	SAMPLE	Q_{mue}	Q_{muu}	Qp_{2-3}	$Qp_{>3}$	Q_{Total}	A	P	F_{total}	L_m	L_v	L_s	L_T	M	D	TOTAL
1	Ns1	130	18	12	11	171	5	9	14	94	7	0	101	8	6	300
2	Ns2	138	16	13	10	177	4	10	14	101	2	0	104	4	1	300
3	Ns3	130	20	10	9	169	3	16	19	104	5	0	109	2	0	300
4	Ns4	150	10	14	5	173	2	12	14	98	6	1	105	3	1	300
5	Ns5	126	30	9	15	180	1	8	9	106	2	0	108	2	1	300
6	M-K1	155	12	6	10	183	0	10	10	112	4	0	116	3	0	300
7	M-K2	170	5	3	30	208	4	9	13	60	15	1	76	2	1	300
8	M-K3	180	10	4	6	200	4	12	14	43	4	0	47	38	1	300
9	M-K4	135	6	7	40	188	6	8	14	50	10	1	61	33	4	300
10	M-K5	160	4	5	25	194	2	10	12	70	1	0	71	20	3	300
11	FZP-1	145	15	4	30	182	7	12	19	60	3	0	63	15	1	300
12	FZP-2	112	8	5	59	184	1	9	10	40	1	0	41	22	2	300
13	FZP-3	142	4	5	20	171	4	18	22	40	6	0	46	14	1	300
14	FZP-4	130	3	10	50	193	3	11	14	49	4	0	53	37	3	300
15	FZP-5	136	4	5	40	185	2	13	15	85	3	0	88	12	0	300

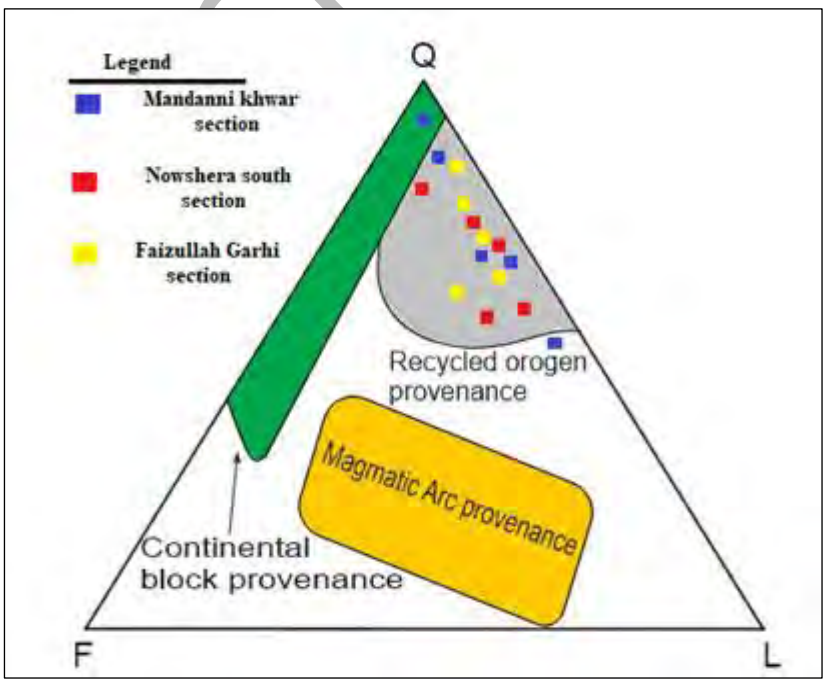

Figure 3.7. Quartz-Feldspar-Lithic fragments plot for the representative samples. Q = Quartz, F = Feldspar and L = Lithic fragments (Dickinson and Suczek, 1979).

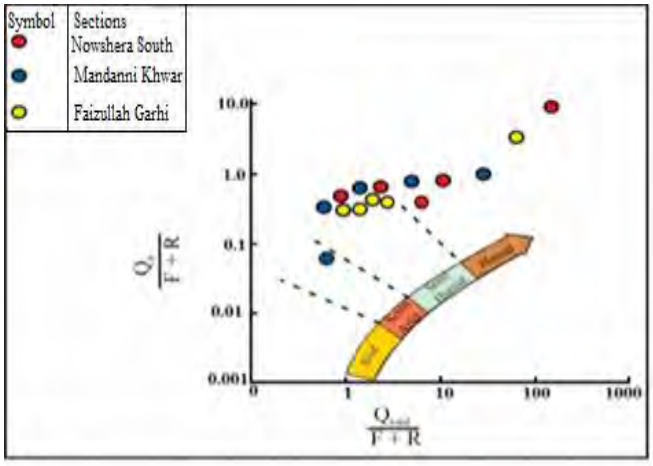

Figure.3.8. Log–log plot of polycrystalline quartz (Q_p/F + R) vs. total quartz Q_{total}/F + R (Suttner and Dutta, 1986). The five samples from the humid zone suggest that clasts derived from the local mature Palaeozoic sedimentary quartzite.

3.4 Geochemical Analyses

For bulk rock geochemistry, 23 samples were crushed and homogenized. Geochemical analysis was conducted using inductively coupled plasma emission spectroscopy/mass spectrometry (ICP-OES; Spectro Ciros Vision). Oxides, major, (Table 3.2) minor, trace, and rare earth elements were among the compounds examined. Each sample was fused in lithium metaborate/tetraborate and digested in nitric acid to extract Si, Nb, and Rb, which were then analysed using inductively coupled plasma optical emission spectrometry. To determine the Al, Fe, Mg, Ca, Na, K, Ti, P, Mn, Cr, Ba, Co, Sr, Th, U, V, W, and Zr, further 0.5 g of each sample was digested in 95°C aqua regia by using ICP-MS (Perkin Elmer ELAN 9000, Sciex). Reference materials were used to calibrate both splits. The depositional paleoenvironments and paleoclimatic conditions during the sediment depositions were reconstructed using several geochemical proxies.

Table 3.2. Major oxides percentage in Mandanni Khwar, Faizullah Garhi proper and Nowshera South sections.

S.No	Samples ID	SiO_2	Al_2O_3	FeO_3	MgO	CaO	Na_2O	K_2O	TiO_2	P_2O_5	MnO	CrO
1	MK-1	60.73	13.58	5.82	2.83	3.96	1.12	2.19	0.73	0.14	0.11	0.015
2	MK-2	58.15	14.26	5.95	2.8	5.4	1.58	2.46	0.91	0.09	0.09	0.019
3	MK-3	51.57	16.55	7.43	3.98	5.94	1.73	2.62	0.78	0.07	0.11	0.017
4	MK-4	50.28	15.37	6.99	3.62	6.47	1.47	2.74	0.65	0.1	0.09	0.018
5	MK-5	48.48	14.48	6.47	3.44	10.6	1.91	2.2	0.76	0.16	0.09	0.017
6	MK-6	24.85	8.44	3.29	2.02	31.1	0.71	1.54	0.6	0.12	0.1	0.018
7	MK-7	46.47	10.84	4.5	3.08	15.17	1.21	1.92	0.8	0.11	0.06	0.012
8	FZP-1	53.24	18.1	6.14	3.19	4.23	1.52	3.68	0.78	0.15	0.1	0.023
9	FZP-2	48.69	19.27	8.37	4.3	2.72	1.12	4.41	0.77	0.16	0.13	0.018
10	FZP-3	49.18	19.08	9.09	4.53	1.88	0.89	4.45	0.74	0.13	0.1	0.016
11	FZP-4	49.98	19.34	7.72	4.63	1.67	0.6	4.19	0.69	0.17	0.12	0.017
12	FZP-5	59.72	14.19	5.52	2.65	4.78	1.46	2.42	0.37	0.07	0.06	0.015
13	FZP-5A	63.16	14.62	5.92	2.45	3.07	2.01	2.48	0.62	0.11	0.06	0.019
14	FZP-6	47.48	14.53	5.21	3	10.93	1.03	2.71	0.62	0.11	0.06	0.017
15	NS-1	67.7	12.74	4.01	1.71	4.58	2.2	2.2	0.5	0.09	0.08	0.018
16	NS-2	68	12.77	4.04	1.8	4.02	2.28	2.23	0.5	0.1	0.07	0.017
17	NS-3	55.46	11.84	4.36	2.12	10.96	1.83	2.02	0.57	0.14	0.08	0.018
18	NS-4	50.16	10.59	3.86	2.01	15.31	1.68	1.84	0.53	0.13	0.06	0.012
19	NS-5	46.82	12.56	4.92	2.85	14.33	1.98	2.35	0.65	0.22	0.08	0.023
20	NS-6	49.35	15.68	6.97	3.74	7.27	2.28	3.17	0.75	0.16	0.11	0.018
21	NS-7	58.41	14.58	5.27	2.94	6.25	2.6	2.78	0.66	0.19	0.09	0.016
22	NS-8	53.87	12.6	5.11	2.83	10.19	1.72	2.16	0.71	0.19	0.09	0.017
23	NS-9	55.12	12.67	5.15	3.05	9.17	1.75	2.22	0.7	0.19	0.09	0.015

Table 3.3. The proportions of trace elements and Loss on Ignition of the studied samples.

S.No	Samples ID	As	Ba	Be	Ce	Co	Cu	Dy	Ga	Gd	Pr	Rb	Sr	Th	Zr	U	LOI
1	MK-1	4.4	515	4	56.1	28.6	39.3	3.98	20.5	4.32	6.38	167.9	158.8	13.1	131.9	3.3	8.7
2	MK-2	6.1	590	2	46	27.4	49.2	2.86	25.7	3.24	5.34	236.8	147.4	14.4	79.5	3.6	9.9
3	MK-3	5.7	638	3	44.1	29.6	47.6	2.62	26.3	3.12	4.96	255.2	135.8	13.7	57.4	2.6	9.5
4	MK-4	5.5	604	3	46.6	30.3	51.1	2.59	27.1	3.04	5.18	239.3	135.4	12.7	75.1	3.4	10.6
5	MK-5	13.4	458	3	66.2	16	31.1	3.68	15.1	4.66	7.27	112.4	201.1	13.2	209	3.9	8.5
6	MK-6	9	411	1	81.1	15.8	38.2	5.37	16	6.17	9.44	111.7	195.4	16.2	244.7	1.8	5
7	MK-7	8.3	474	4	46.1	13.7	30.3	3.69	15.7	3.89	5.38	124.1	167.4	10.6	125.8	3.2	14.1
8	FZP-1	8.8	392	5	90.6	16.7	25.4	5.55	15.9	6.31	10.02	114.6	167.7	17.3	315.8	2.8	8.5
9	FZP-2	9	462	3	91.9	17.7	34.2	5.56	16.5	6.87	10.39	112.5	236.6	19.8	257.8	2.6	8.1
10	FZP-3	9.4	655	1	53.2	24.2	67.9	3.72	18.7	4.44	6.31	130	295.7	12.6	113.5	3.3	8.9
11	FZP-4	11.4	650	3	64.1	21.9	48.6	4.32	18.3	4.77	7.22	136.6	204.9	14.6	121.7	2.1	11.8
12	FZP-5	13.2	432	1	60.6	19.6	53.9	3.86	16.2	4.55	6.9	110.2	310	14.4	136.8	2.4	11.2
13	FZP-5A	7.9	324	1	33	11.3	25.1	3.13	9.6	3.38	4.72	76.1	615.9	7.9	70.5	3.7	27.4
14	FZP-6	9.4	381	1	64.8	13.7	24.6	4.49	12.2	5.34	7.66	87.4	436.8	13.1	213.4	1.9	15.8
15	NS-1	4.7	334	3	54.8	9.4	13.6	3.38	13.7	3.7	6.1	88.7	218.1	10.6	131.3	1.5	4
16	NS-2	4.8	344	3	58.8	8.9	13.1	3.6	13.3	3.89	6.26	97.2	200.3	10	152.1	1.9	4
17	NS-3	6.1	360	1	59.6	10.6	17.7	4.06	12.7	4.38	6.77	85.8	214.6	10.5	182.3	2.3	10.4
18	NS-4	5.6	317	2	59.6	10	17.2	3.98	11.7	4.49	6.77	82.8	224	10.8	208.2	2.6	13.7
19	NS-5	6.7	415	3	74.9	17.1	34.9	5.19	13.8	5.92	9.24	103.8	276.2	17.2	197.6	3.6	13
20	NS-6	6.5	536	2	63.2	19	52.9	3.89	19.6	4.49	6.95	160.2	216.7	15.2	109.5	3.5	10.3
21	NS-7	6.5	537	2	67.5	13.5	36.9	3.98	16.3	4.64	7.54	125	280.4	15.8	173.2	2.7	6
22	NS-8	9.3	396	1	83.8	14	29	5.3	13.6	6.13	9.41	91.3	258.9	15.8	282.4	3.5	10.3
23	NS-9	9.7	394	2	74.1	14.4	28	4.89	13.8	5.43	8.52	96.2	275.7	14.7	249.4	3	9.7

3.4.1 Chemical Index of Alteration (CIA)

The CIA is a measurement of how sediments are weathered. CIA is a reliable paleoclimatic indicator (Nesbitt and Young, 1982, 1984, Taylor and McLennan, 1985; Yan et al., 2010).

CIA= $\frac{Al2O3}{(Al2O3 + CaO + Na2O+K2O)} \times 100$ and formula of PIA=$100 \times \frac{(Al2O3 - K2O)}{(Al2O3 + CaO* + Na2O- K2O)}$The highest values of CIA in study sections 75, (Table 3.4) for the bentonite rich clay, while the CIA values of sand-silt-clay is 59.0 and the loess deposits having 50.2 values. The CIA value is high in the Mandanni Khwar and Faizullah Garhi. The PIA having a similar tendency to the CIA with the

sand–silt–clay rhythmites displaying an average of 78.6 and the loess deposits have 77.5 in average. The lowest value is 55.3 correspond to coarse sand.

Table 3.4. Chemical Index of Alteration (CIA) values table for study sections

Samples ID	Al_2O_3	CaO	Na_2O	K_2O	Al_2O_3+ CaO+ Na_2O+ K_2O	CIA
MK-1	13.58	3.96	1.12	2.19	20.85	65.13
MK-2	14.26	5.4	1.58	2.46	23.7	60.21
MK-3	16.55	5.94	1.73	2.62	26.84	61.66
MK-4	15.37	6.47	1.47	2.74	26.05	59.00
MK-5	14.48	10.6	1.91	2.2	29.19	50.00
MK-6	8.44	31.1	0.71	1.54	41.79	20.20
MK-7	10.84	15.17	1.21	1.92	29.14	37.21
FZP-1	18.1	4.23	1.52	3.68	27.53	66.00
FZP-2	19.27	2.72	1.12	4.41	27.52	70.03
FZP-3	19.08	1.88	0.89	4.45	26.3	73.04
FZP-4	19.34	1.67	0.6	4.19	25.8	75.00
FZP-5	14.19	4.78	1.46	2.42	22.85	62.00
FZP-6	14.62	3.07	2.01	2.48	22.18	66.03
FZP-7	14.53	10.93	1.03	2.71	29.2	50.23
NS-1	12.74	4.58	2.2	2.2	21.72	58.65
NS-2	12.77	4.02	2.28	2.23	21.3	60.00
NS-3	11.84	10.96	1.83	2.02	26.65	44.42
NS-4	10.59	15.31	1.68	1.84	29.42	36.00
NS-5	12.56	14.33	1.98	2.35	31.22	40.23
NS-6	15.68	7.27	2.28	3.17	28.4	55.21
NS-7	14.58	6.25	2.6	2.78	26.21	55.62
NS-8	12.6	10.19	1.72	2.16	26.67	47.24
NS-9	12.67	9.17	1.75	2.22	25.81	49.08

3.4.2 Plagioclase Index of Alteration (PIA)

The plagioclase index of alteration can be calculated with formula, $PIA=100*\frac{(Al2O3 - K2O)}{(Al2O3 + CaO* + Na2O - K2O)}$.The weathering grade of plagioclase is also determined by the Plagioclase index of alteration (Fedo et al., 1995).The PIA having a similar tendency to the CIA with the sand–silt–clay rhythmites of Mandanni Khwar sections display maximum values (86.9) of PIA in sample MK-4 (Table 3.5) and the loess deposits have 50.3. The lowest value is 17.8 correspond to coarse sand of Faizullah Garhi section.

Table 3.5. Plagioclase Index of Alteration (PIA) values table of studied sections.

Samples ID	Al_2O_3	CaO	Na_2O	K_2O	Al_2O_3-K_2O	Al2O3+CaO+Na2O	PIA
MK-1	13.58	3.96	1.12	2.19	11.39	18.66	69.1
MK-2	14.26	5.4	1.58	2.46	11.8	21.24	62.8
MK-3	16.55	5.94	1.73	2.62	13.93	24.22	64.4
MK-4	15.37	6.47	1.47	2.74	12.63	23.31	61.4
MK-5	14.48	10.6	1.91	2.2	12.28	26.99	49.5
MK-6	8.44	31.1	0.71	1.54	6.9	40.25	17.8
MK-7	10.84	15.17	1.21	1.92	8.92	27.22	35.2
FZP-1	18.1	4.23	1.52	3.68	14.42	23.85	71.4
FZP-2	19.27	2.72	1.12	4.41	14.86	23.11	79.4
FZP-3	19.08	1.88	0.89	4.45	14.63	21.85	84.0
FZP-4	19.34	1.67	0.6	4.19	15.15	21.61	86.9
FZP-5	14.19	4.78	1.46	2.42	11.77	20.43	65.3
FZP-6	14.62	3.07	2.01	2.48	12.14	19.7	70.4
FZP-7	14.53	10.93	1.03	2.71	11.82	26.49	49.7
NS-1	12.74	4.58	2.2	2.2	10.54	19.52	60.8
NS-2	12.77	4.02	2.28	2.23	10.54	19.07	62.5
NS-3	11.84	10.96	1.83	2.02	9.82	24.63	43.4
NS-4	10.59	15.31	1.68	1.84	8.75	27.58	33.9
NS-5	12.56	14.33	1.98	2.35	10.21	28.87	38.4
NS-6	15.68	7.27	2.28	3.17	12.51	25.23	56.7
NS-7	14.58	6.25	2.6	2.78	11.8	23.43	57.1
NS-8	12.6	10.19	1.72	2.16	10.44	24.51	46.7
NS-9	12.67	9.17	1.75	2.22	10.45	23.59	48.9

3.4.3 Al_2O_3 vs. CIA plot

Al_2O_3 vs. CIA plot (Goldburg and Humayun, 2010) show a group of samples in the ranges of 1-2. The range of Al_2O_3 is 8.44 to 19.27. The bentonite rich clay has high content of Al_2O_3 as compared to loess deposits. Therefore, the bentonite rich clay samples of Mandanni Khwar section and Faizullah Garhi section are slightly separated from Nowshera south section. (Fig. 3.9)

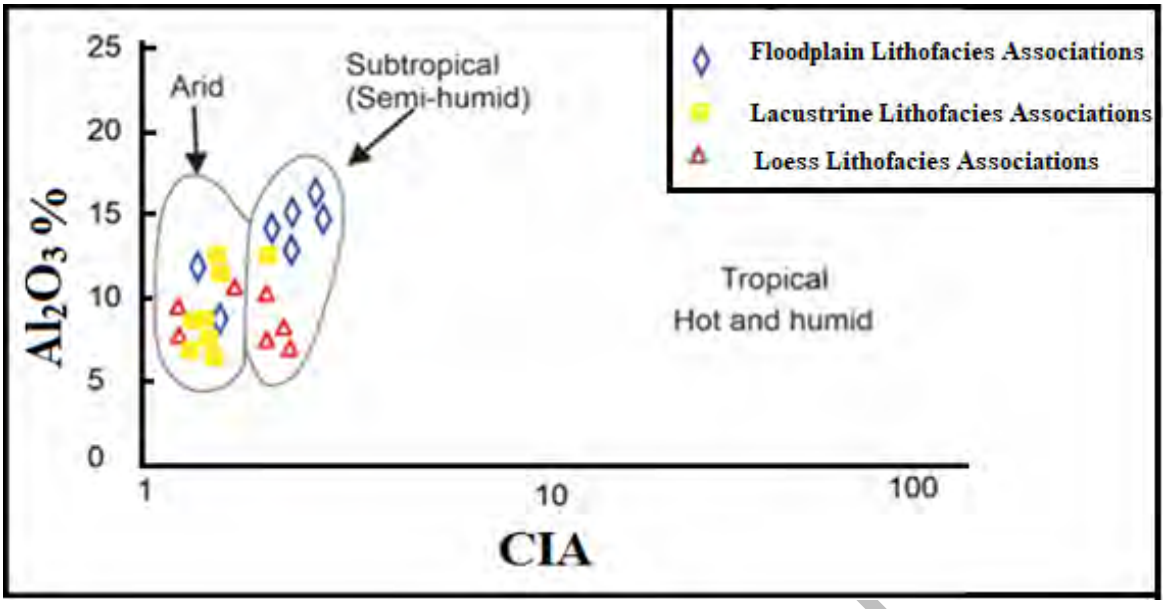

Figure 3.9. Al2O3 % versus Chemical Index of Alteration (CIA) plot for the representative samples (after Goldburg and Humayun, 2010).

3.4.4 K_2O/Na_2O versus CIA plot

This plot having samples distribution like Al_2O_3 vs. CIA plot. Due to high content of K_2O the bentonite rich clays have slightly high ratios as compared to loess deposits (Fig. 3.10)

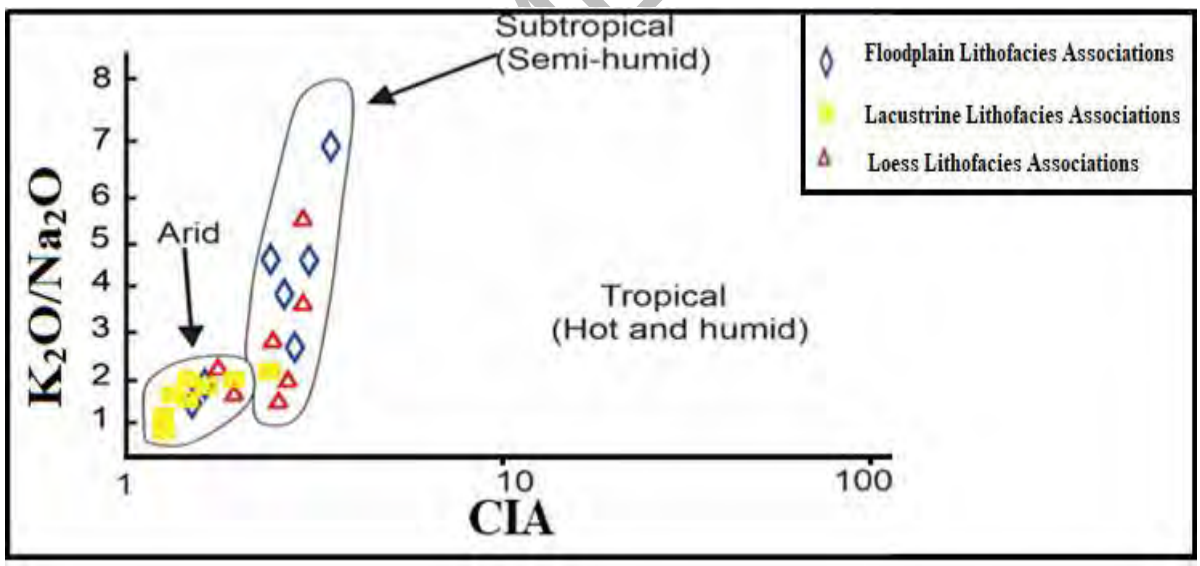

Figure 3.10. Plot of chemical index of alteration versus K_2O/Na_2O (after Goldburg and Humayun, 2010).

3.4.5 A–CN–K plot

The A-CN-K is ternary plot of Al_2O_3 (A), CaO*+Na_2O (CN), and K_2O (K). The study sections samples show a bunch along the line of A-CN sides, while some loess deposits samples due to high contents of CN plot on the lower part close to CN climax of triangle (Fig. 3.11) All the

selected samples lie below the smectite-illite line. The ranges of samples are started from upper continental crust (UCC) and faintly away from average continental crust (ACC). The bentonite rich-clays samples of Faizullah Garhi proper have higher position like Post-Archaean Australian Shale (PAAS).

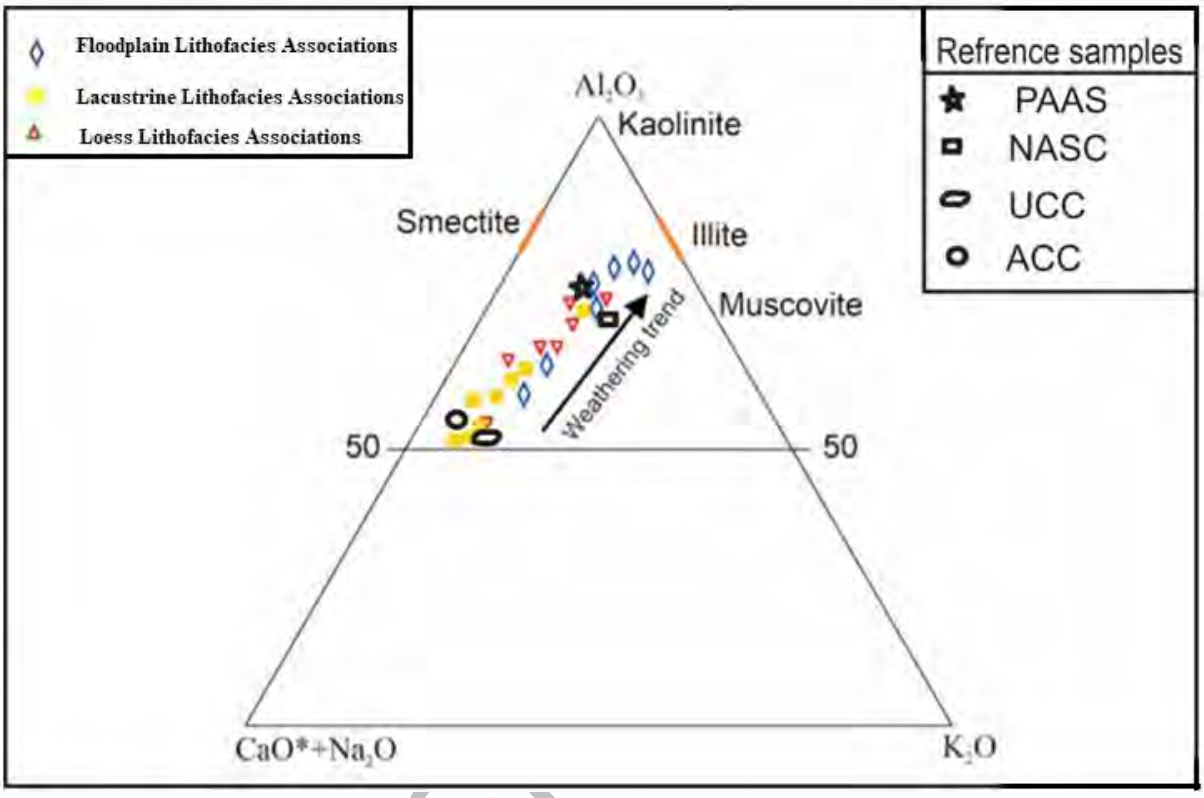

Figure 3.11. A–CN–K plot for the representative samples, positions of reference minerals (muscovite, illite, smectite, and kaolinite) are given. CaO* = Calcium oxide content in the silicate component (Basu, A. 1976)

The Lacustrine Fluvial Lithofacies Associations and Loess Lithofacies Associations occupy a close position to the UCC and ACC while the FPLA samples are close to PAAS and NASC. UCC = Upper Continental Crust, ACC = Average Continental Crust, PAAS = Post-Archaean Australian Shales, NASC = North American Shale Composite.

3.4.6 Chemical maturity proxy plot

The amount of Al, Si, K, and Na in sediments is controlled by mineralogical differences in the parent rock composition. Using the SiO_2 versus total $Al_2O_3 + K_2O + Na_2O$ plot (Malick and Ishiga, 2016; Suttner and Dutta, 1986) (Fig. 3.12) the chemical maturity trend of siliciclastic can be established.

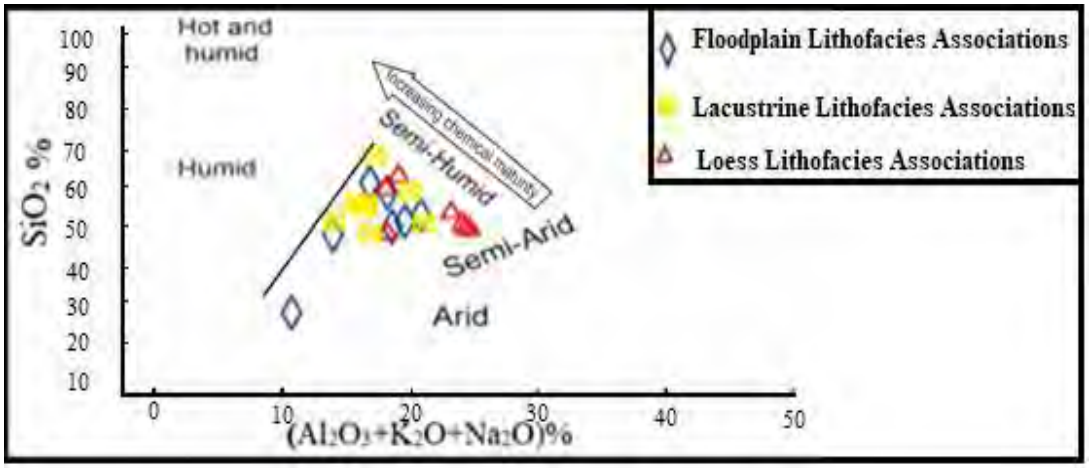

Figure 3.12. Chemical maturity proxy plot for SiO_2 versus $Al_2O_3+K_2O+Na_2O$ (Malick and Ishiga, 2016; Suttner and Dutta, 1986). showing paleoclimatic conditions during the deposition.

Chapter 4

Interpretation and Discussion

Introduction

This chapter comprises the interpretation and discussion based on the results of the data set described in chapter 3. This interpretation of the data set is comprised of three phases. The first phase is the lithofacies analysis and their associations, the second phase is petrography, and the third phase is the geochemical composition of the studied sections.

4.1 Sedimentology and Lithofacies Correlations

The Pleistocene–Holocene strata of the Peshawar Basin have been categorized into the following lithofacies classes and facies relationships, based primarily on field observations.

4.1.1 Conglomerate Lithofacies/Alluvial Fan Lithofacies

The conglomerate lithofacies contains a poorly sorted conglomerate in the basal part of the studied sections. The thickness of Conglomerate Lithofacies is 9m. The Faizullah Garhi, Mandanni Khwar sections, and Nowshera South sections have many strata of poorly sorted conglomerates. The conglomerates of the Faizullah Garhi area are made up of poorly sorted clasts of limestone, sandstone, and shale. Limestone clasts suggest sedimentation from a consistent source of carbonate formations exposed in the western part of the Attock–Cherat Ranges and adjacent MBT-related ridges. The Faizullah Garhi section has a clast-supported framework with a majority of subrounded to relatively well-rounded clasts, with crude clast imbrications parallel to the bedding planes, indicating fluvial stream transportation. In the Nowshera South section, the conglomerates have dominancy of slaty clasts which support the fluvial influence. The predominance of slate clasts indicates debris supply from the Manki Formation. Strong reworking and sediment mixing under abnormally high energy circumstances are shown by the presence of locally generated angular

clasts. (Fig. 4.1). The immaturity of the dominating conglomerates textures shows that they were formed by immature sedimentary processes. These kinds of situations are common in alluvial plains, where sediments are deposited by gravity near to elevated source sites.

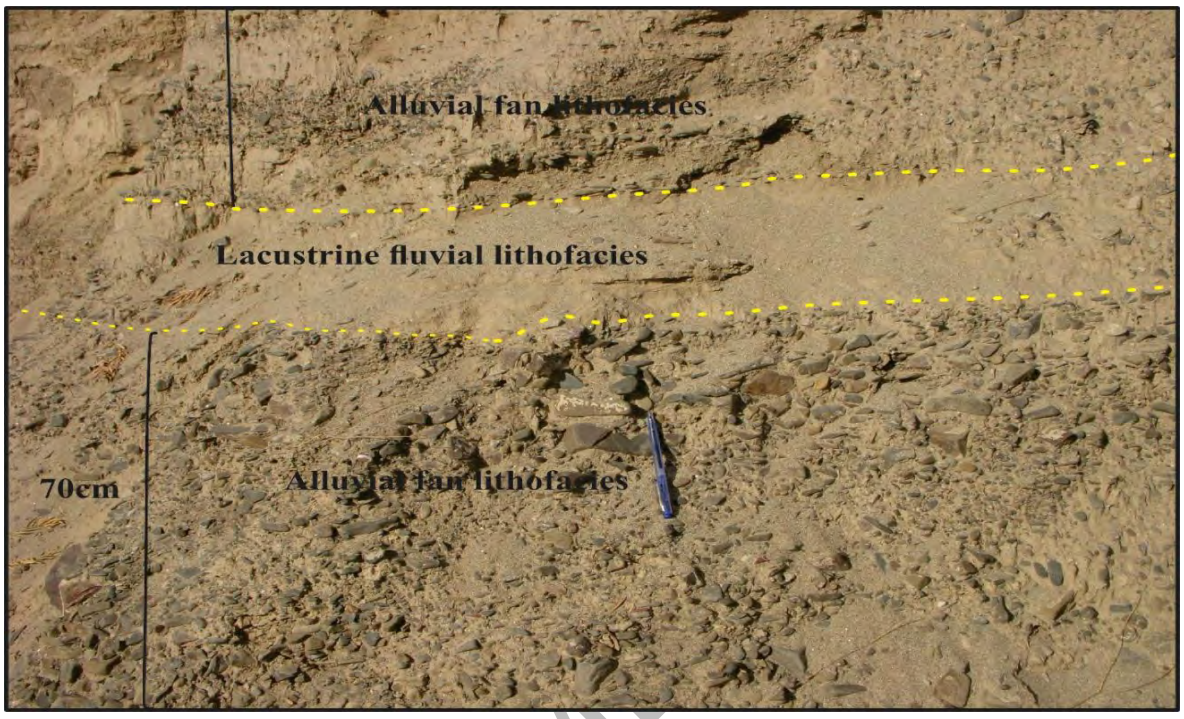

Figure 4.1. Alluvial fan lithofacies and lacustrine fluvial lithofacies at Nowshera south section.

4.1.2 Interbedded Claystone and Siltstone Lithofacies/Floodplain Clay Lithofacies

Interbedded claystone and siltstone lithofacies are composed of interbedded claystone and siltstone. This lithofacies has clayey cycles rich in bentonites in the lower part of studied sections (Fig. 4.2). This lithofacies has fine grain clay and silt of each cycle, as well as the planar bedding planes, indicating that argillites were deposited on a relatively flat area. The absence of coarse-grained debris eliminates high-energy deposition conditions. Only argillites were shed during the flood season, thus it supports that deposition occurs in a floodplain situation.

Figure 4.2. Interbedded claystone and siltstone lithofacies of Mandanni Khwar section.

4.1.3 Interbedded Sand and Silt Lithofacies/Lacustrine-Fluvial Lithofacies

This lithofacies is distinguished by the presence of sand, silt, and scattered pebbles (Fig. 4.3) from interbedded claystone and siltstone lithofacies of the Mandanni Khwar section. Deposition as crevasse splays is supported by the fining upward character, wavy bedding designs, and pinching out of beds. Low-lying areas and abandoned channels were filled during the periodic breakout floods, resulting in ponds and lakes in various parts of the basin that were gradually filled with rhythmites (Cornwell, 1998). The absence of red clay tops/paleosols and mud cracks, on the other hand, indicate significant subaerial exposure and support the concept of deposition in a more stable, huge lake caused by the uplifting of the Attock-Cherat Range. (Pivnik and Johnson, 1995).

4.1.4 Loess Lithofacies

The loess lithofacies occur in the upper part of the studied section. The Loess lithofacies constitute the youngest depositional phase, which is formed mostly by windblown transportation. The thickness of these lithofacies is 2m, 5m, and 5.4m in Mandanni Khwar, Faizullah Garhi, and the Nowshera South section. The presence of calcrete concretions and carbonate horizons shows that the sediment was deposited in arid settings with poor chemical weathering. The absence of paleosols suggests a lack of soil-forming processes, which is common in cold, glacial environments.

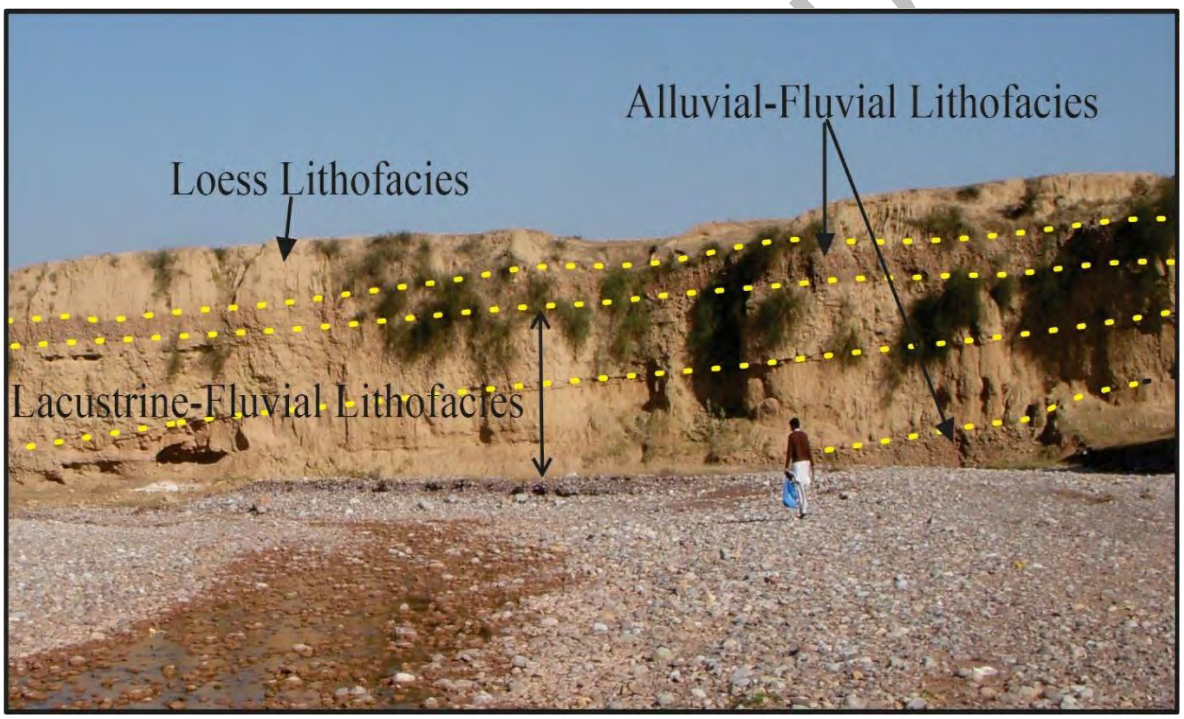

Figure 4.3 Alluvial fan lithofacies, Loess Lithofacies, and Lacustrine-Fluvial Lithofacies at Mandanni Khwar section.

4.2 Lithofacies Associations

Three separate lithostratigraphic sections were investigated and used to generate and analyze facies based on sedimentological and lithological factors. Facies that were genetically related (based on origin and process) were then grouped to form facies associations. Following that, genetically similar (based on origin and process) facies were grouped to construct facies associations, which

were utilized to determine the Paleoclimate variation and weathering trend in the analyzed sections. The following lithofacies associations were established.

4.2.1 Floodplain Clay Lithofacies Association (FCLA)

The Floodplain Clay Lithofacies Associations (FCLA) comprise the floodplain clay lithofacies, which occupy the lowest position in examined sections. The largest exposed thickness of FCL is 11 m in the Faizullah Garhi and Mandanni Khwar sections. This FCLA has fine-grain clay and silt in each cycle, as well as the planar bedding planes, which indicates that argillites were deposited on a relatively flat area. Only argillites were shed during the flood season, thus it supports that deposition occurs in a floodplain situation. Subaerial exposure is indicated by the presence of loess in the upper section.

4.2.2 Lacustrine Fluvial Lithofacies Association (LFLA)

The Lacustrine Fluvial Lithofacies Association (LFLA) contains the lacustrine fluvial floodplain lithofacies (LFL) and alluvial fan lithofacies (AFL) in studied sections. Lacustrine fluvial floodplain lithofacies is distinguished by the presence of sand, silt, and scattered pebbles from Floodplain clay lithofacies of Mandanni Khwar section. Alluvial fan lithofacies (AFL) in Faizullah Garhi, Mandanni Khwar and Nowshera sections have poorly sorted conglomerates. The conglomerates of the Faizullah Garhi area are made up of poorly sorted clasts of limestone, sandstone, and shale. The predominant conglomerates' textural immaturity implies formation by immature sedimentary processes. Such situations are common in alluvial plains, where sediments are deposited by gravity near elevation source locations (Boggs, 2009).

4.2.3 Loess Lithofacies Association (LLA)

The Loess Lithofacies Association (LLA) is made up of a series of loess lithofacies. In all the studied sections, the relationship is uniformly developed. The maximum thickness is reported in

Nowshera South section is 5.4 meters. The presence of calcrete concretions and carbonate horizons shows that the sediments were deposited in arid settings with poor chemical weathering.

Table 4.1. Summary, field features, lithofacies, and lithofacies associations of study sections.

Lithofacies	Field features	Interpretation	Lithofacies association
Alluvial Fan Lithofacies	Immature conglomerate having limestone and Manki slate clasts.	clast imbrications parallel to the bedding planes, indicating fluvial conditions.	
Lacustrine Fluvial-Floodplain Lithofacies	Presence of sand, silt, and scattered pebbles. pinching out of beds	Deposition in low laying area and lake.	**Lacustrine Fluvial Lithofacies associations**
Floodplain Clays Lithofacies	Thin lamination. Bentonite rich clay.	Floodplain setting deposits.	**Floodplain clay lithofacies**
Loess lithofacies	Unstratified red clay, carbonate horizon, having maximum thickness.	The deposition occurs at the arid condition with little chemical weathering.	**Loess lithofacies associations**

4.3 Petrographic studies

Thin sections of 15 samples from Mandanni Khwar, Faizullah Garhi and Nowshera South sections were studied. Modal analysis of thin sections was carried out with the help of Image Analysis software. The most common clastic grain is quartz, which comes in monocrystalline (Q_m) and polycrystalline (Q_p) variants. Q_{total} contributes for 54 % of the framework's components on average. Q_{mue} is the most common, accounting for 35 % of the total framework composition, followed by Q_{muu} (7%), with Q_{pq} (2–3) content accounting for 3% and $Q_{pq} > 3$ accounting for 6.9%.

According to the QFL triangular diagram the sediments were produced from a recycled orogenic belt (Fig. 4.4) and deposited in cold paleoclimate. There is no sediment mixing from either a magmatic or sedimentary block, and the high concentration of L, Q, and F implies poor chemical weathering.

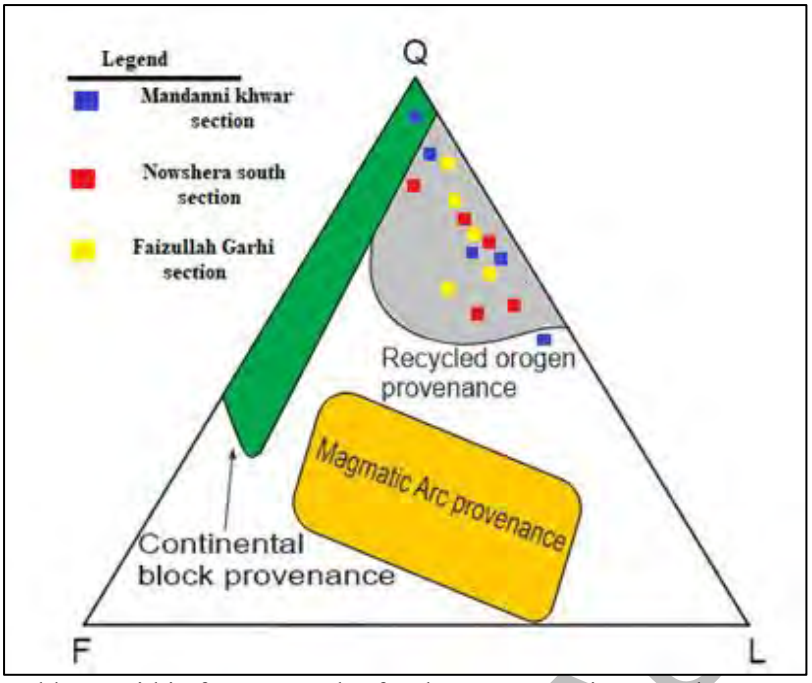

Figure. 4.4 Quartz-Feldspar-Lithic fragments plot for the representative samples. Q=Quartz, F= Feldspar and L=Lithic fragments. (Dickinson and Suczek, 1979).

In log/log plot of Q_P/ (F + R) versus Q_{total}/ (F + R) samples cluster come in the semi-arid to semi-humid part of the plot, which shows that sediments were produced under relatively mild weathering conditions, allowing feldspars and other heavy minerals to be preserved (Suttner and Dutta, 1986). Five samples in the humid zone show relic of a mature source in the Peshawar Basin in the form of Palaeozoic rocks (most probable Misri Banda Quartzite).

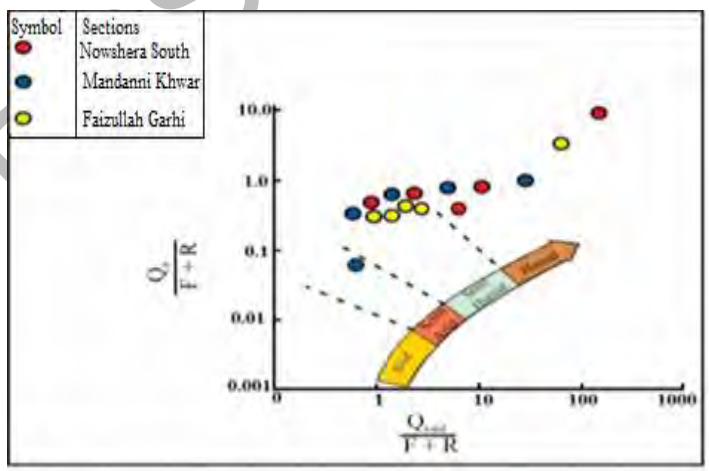

Figure.4.5. Log/log plot of polycrystalline quartz (Qp/F + R) vs. total quartz Qtotal/F + R (Suttner and Dutta, 1986). The five samples from the humid zone suggest that clasts derived from the local mature Palaeozoic sedimentary quartzite.

4.4 Geochemical analysis

Geochemical proxies were used to interpret paleoclimatic condition and weathering trend during the sediment's depositions based on work by for example, Fischer and Wefer (2012); Hofmann et al., (2001); Iqbal et al., (2019).

4.4.1 Chemical Index of Alteration

The Chemical Index of Alteration (CIA) has been used to measure the weathering history of sedimentary rocks, with the goal of better understanding paleoclimate conditions (Nesbitt and Young, 1982, 1984). A CIA number between 50 and 60 denotes a modest degree of chemical weathering, a CIA value between 60 and 80 represents moderate chemical weathering, and a CIA value between 80 and 100 represents significant chemical weathering, according to a study by (Fedo et al., 1995). The highest value of CIA studied sections is 75, (Table. 3.4) for the bentonite-rich clay, while the CIA average value of sand-silt-clay is 59.2, and the loess deposits have average value 49.8.

The Floodplain clay lithofacies of the Mandanni Khwar section and Faizullah Garhi section with relatively high CIA values designate an increasing trend in chemical weathering but still under mainly cold-arid conditions. While the low CIA values for the loess lithofacies imply that chemical weathering was quite low during sedimentation (Bahlburg and Dobrzinski, 2011). Similarly, the Lacustrine Fluvial Lithofacies associations have low CIA values, which indicate the deposition in a cold, dry environment.

4.4.2 Al_2O_3 vs. CIA plot

The scaled Al_2O_3 vs CIA scattered plot (Fig. 4.6) (Goldberg and Humayun, 2010) suggests sedimentation in arid paleoclimate. The close population cluster in the low Al_2O_3 and extremely low CIA regions suggests that uniform conditions are dominated by poor chemical weathering. The Floodplain Lithofacies Associations samples, on the other hand, have slightly higher Al_2O_3 and CIA, indicating a subtropical (semiarid–subhumid) paleoclimate.

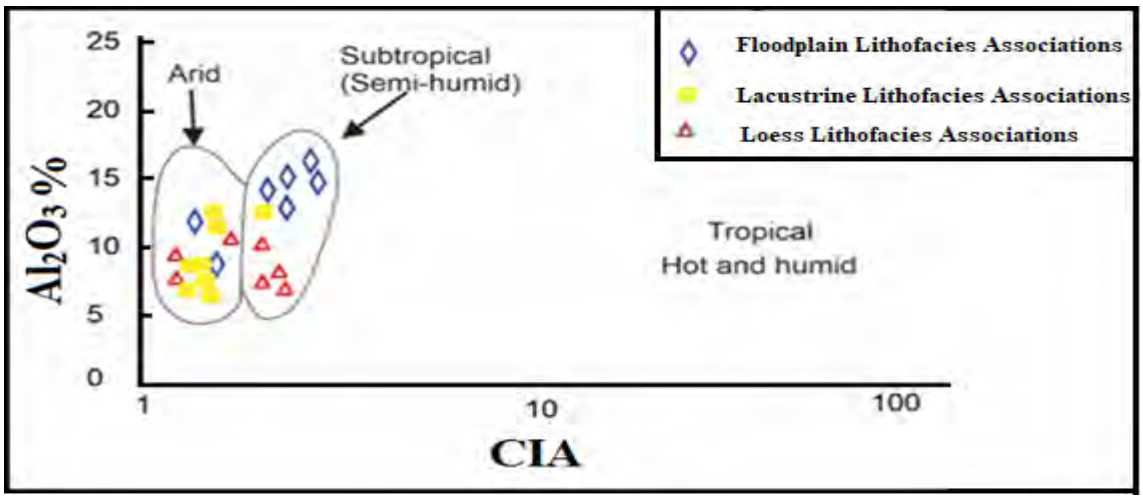

Figure 4.6. Al_2O_3 % versus Chemical Index of Alteration (CIA) plot for the representative samples (after Goldburg and Humayun, 2010).

4.4.3 K_2O/Na_2O versus CIA plot

The scattered plot of scaled K_2O/Na_2O versus CIA (Fig. 4.7) (Goldberg and Humayun, 2010) suggests sedimentation in an arid paleoclimate. The proximity of the population clusters in the low K_2O/Na_2O and extremely low CIA regions suggests that uniform conditions are dominated by poor chemical weathering. In contrast, the Floodplain clay lithofacies of Mandanni khwar and Faizullah Garhi sections samples have slightly higher K_2O/Na_2O and CIA values, indicating a subtropical (semiarid–subhumid) paleoclimate.

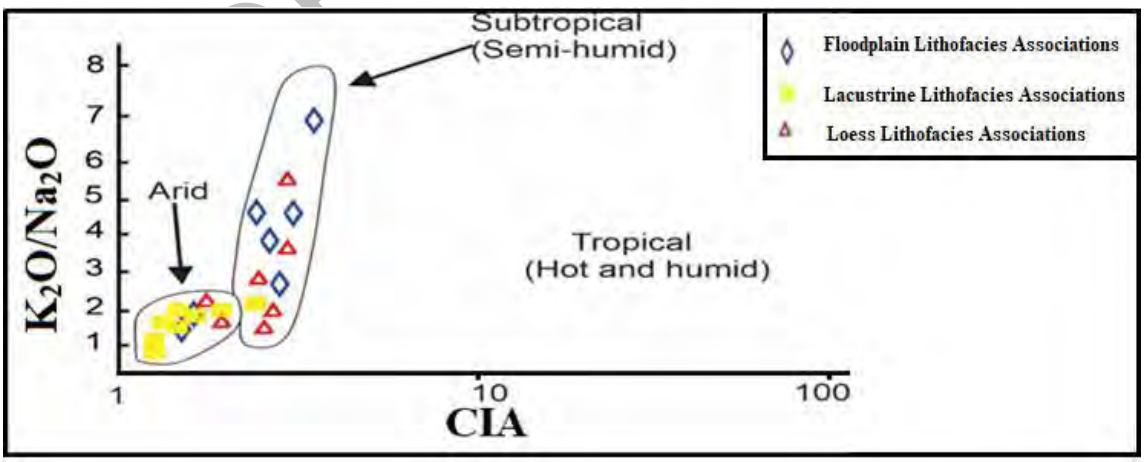

Figure 4.7. Plot of chemical index of alteration versus K_2O/Na_2O (after Goldburg and Humayun, 2010).

4.4.4 A-CN-K Plot

The A-CN-K diagram can be used to assess the weathering history of the studied samples. The A–CN–K ternary diagram explains the weathering trends of the sediments (Selvaraj and Chen, 2006; Selvaraj et al., 2004). The sample population cluster parallels to the A–CN side favours the sediments' immature nature. All the samples show weathering below the smectite-Illite position, implying that chemical weathering is insignificant. The LFLA and LLA strata plot near the CN apex, while the FPLA strata plot near the A apex. (Fig. 4.8).

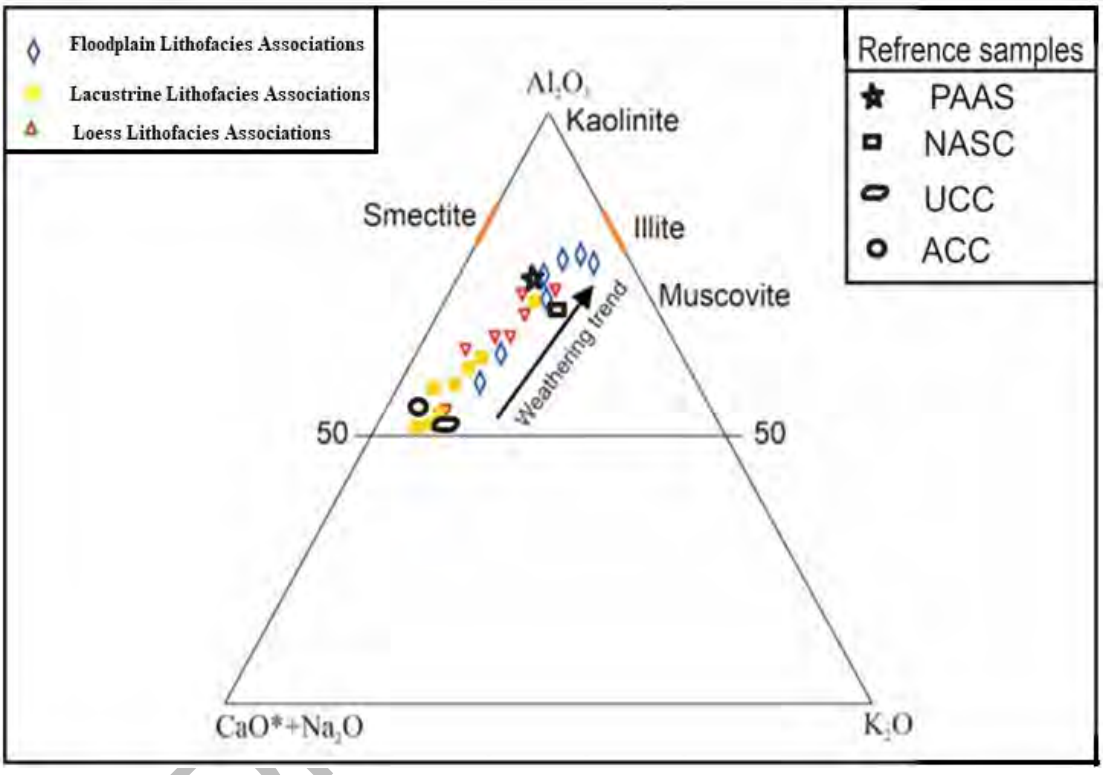

Figure 4.8. A–CN–K plot for the representative samples, positions of reference minerals (muscovite, Illite, smectite, and kaolinite) are given. CaO* = Calcium oxide content in the silicate component. UCC = Upper Continental Crust, ACC = Average Continental Crust, PAAS = Post-Archaean Australian Shales, NASC = North American Shale Composite.

The LFLA and LLA occupy a close position to the UCC and ACC while the FPLA samples are close to PAAS and NASC. The loess lithofacies samples due to high contents of CN plot on the lower part close to the CN climax of the triangle (Fig. 4.8). The ranges of samples are started from upper continental crust (UCC) and faintly away from average continental crust (ACC). The bentonite rich-clays samples of Faizullah Garhi have higher position like Post-Archaean Australian Shale (PAAS).

4.4.5 Chemical maturity proxy plot

The diagram of SiO_2 versus Al_2O_3 + Na_2O+K_2O suggests sedimentation in an arid to semiarid paleoclimate. This region's close population samples rule out an extremely humid paleoclimate. The semiarid region is occupied by FPLA, which has a relatively higher CIA and a higher position in the A–CN–K diagram and other geochemical proxies. The LLA which reflects immature positions on all other geochemical proxies' plots occupies position in semi-humid position (Fig. 4.9).

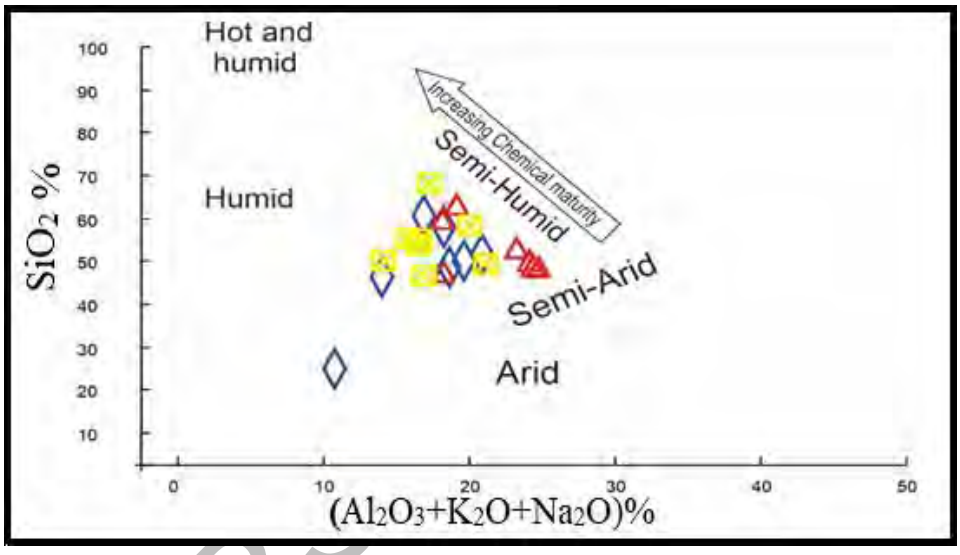

Figure 4.9. Chemical maturity proxy plot for SiO_2 versus Al_2O_3+K_2O+Na_2O (Malick and Ishiga, 2016; Suttner and Dutta, 1986). showing paleoclimatic conditions during the deposition.

4.4.6 Paleoclimate Interpretation

Bentonite-rich clays of the FPLA in the lower portion, sand–silt–clay rhythmites of the LFLA in the middle, and unstratified loess of the LLA at the top compose the Pleistocene–Holocene strata of the Peshawar Basin. The sediments are comprised of immature sand, silt, and clay with boulders/conglomerate intervals that are texturally and compositionally immature. The smectite-Illite rich clay mineralogy, immature sample positions on QFL plots (Fig. 4.4) low CIA values (Table 3.4), (Buggle, Glaser, Hambach, Gerasimenko, and Marković, 2011) and combined geochemistry plots all support sedimentation with insignificant chemical weathering.

Higher field locations on the A–CN–K diagram just next to PAAS (Fig. 4.8) and subtropical (semi-humid) field positions support paleoclimates that were warmer and more humid. The FPLA has an arid paleoclimate, as per the compositional maturity proxy plot. With low CIA values, lower position on the A–CN–K plot near UCC, and arid field position on the paleoclimatic plots, the overlying LFLA indicates cold, arid climate sedimentation. Low kaolinite content is also linked to poor kaolinization and, as a result, reduced chemical weathering. The paleoclimatic proxy plots in the semi-arid to semi-humid zone, on the other hand, indicate considerable seasonality in sedimentation. This indicates that the LFLA was most likely formed in a cool paleoclimatic environment.

On the geochemical proxy plots, (Fig. 4.9) the LLA samples support a paleoclimate interpretation that is like the LFLA. Their arid position on the paleoclimatic proxy plots suggests a dry paleoclimate during deposition, with aeolian transport processes dominating. The presence of multiple calcrete horizons excludes decalcification. The LLA is the result of a cold-arid, wind-dominated paleoclimate.

4.4.7 Weathering trend

To determine the relationship between mineral composition, source rocks, and weathering path, the ternary plot of Al_2O_3 - ($CaO+Na_2O$) - K_2O was used to deduce weathering trends. Nesbitt and Young (1982, 1984, 1989) used a ternary diagram of Al_2O_3 - CaO - K_2O to determine the degree of weathering. In Al_2O_3 - ($CaO+Na_2O$) - K_2O diagram all the samples are plotted below the smectite-Illite position which indicate insignificant weathering. (Fig. 4.8) Lacustrine sediments show slightly more weathering during deposition than loess and floodplain clay samples, supporting the Th/U vs. U plot in their interpretation of weathering trends.

For most rocks, the Rb/Sr ratio rises as the degree of chemical weathering rises. This is because Rb+, is a significant alkali trace element, remains fixed in the weathered residue rather than being

selectively leached like Sr^{2+} (Nesbitt et al., 1980; McLennan et al., 1993). As a result, the Rb/Sr ratio has been utilized to analyse chemical weathering intensity. Rb/Sr > 1 denotes a prominent level of chemical weathering, while Rb/Sr <1 denotes a moderate to low level of chemical weathering. The Rb/Sr ratios in the examined samples range from 0.20 to 0.93 (average: 0.53), indicating low to a modest degree of chemical weathering at the sediment source. Weathering causes the oxidation and subsequent dissolution of U, causing the Th/U ratios to rise above the top crustal values. Other sedimentary processes, on the other hand, may result in U enrichment, lowering the Th/U ratio; in such situations, a low Th/U ratio will be accompanied by a high U content. The Th/U ratio for the upper crustal crust is normally around 3.5 to 4.0. (McLennan et al., 1993). In the present case, the value increases above 3.5-4.0 and reaches up to 6.9. (Fig. 4.10). The average value of Th/U is 5.0, which indicates insignificant chemical weathering during the Plio-Pleistocene in the study sections.

Above the UCC, the loess deposits and floodplain clays show no considerable fractionation, and the lacustrine sediments show little enrichment and weathering.

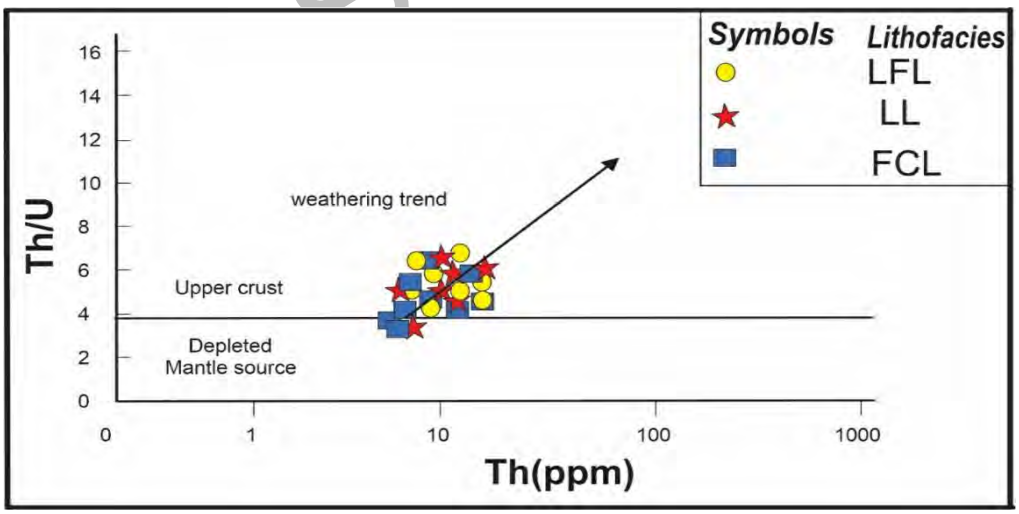

Figure 4.10. Th(ppm) vs Th/U plots (McLennan, 1993) indicates a low degree of weathering of studied sections.

Summary and Conclusion

Summary

The Plio-Pleistocene sedimentary archives are represented in the Peshawar Basin, Pakistan, by an interbedded sequence of mostly sand, silt, and clay rhythmites with interbedded conglomerate and overlain by continuous loess. The Plio-Pleistocene weathering trend, as well as the history of the sediment supply, basin development, climate fluctuation and its effects on sedimentation, are all preserved in the sedimentary archives found within the Basin. The Kabul-Swat Rivers and their nearby tributaries were the main detritus transportation agents during the Plio-Pleistocene and Holocene, according to the present study's bulk sediment geochemical proxies. The sequence indicates Basin formation in response to the Attock-Cherat uplift and maintains paleoclimatic indications during sedimentation. Clays rich in bentonite make up the lowermost portion, while fine-grained siliciclastic deposits in floodplain environments during a slightly mild interglacial period make up the upper portion.

The high concentration of L, Q, and F indicates poor chemical weathering. The QFL triangular diagram indicates that the sediments were formed from a recycled orogenic belt and deposited in a cold climate. Sediments were produced under relatively mild weathering conditions, allowing feldspars and other heavy minerals to be preserved.

The relationship between alkali and alkaline earth elements used to determine the degree of weathering in sedimentary rocks. The labile elements (Na, Ca, and Sr) leach relatively little in the weathering profile, leaving the insoluble elements (Al, Ba, Rb) behind. These chemical changes are transferred to the sedimentary record, providing a useful tool for monitoring source area weathering conditions. Higher values of Al_2O_3, K_2O/Na_2O, and Ba, Al, Rb, and other elements and minerals indicate a subtropical (semiarid–subhumid) paleoclimate.

The Chemical Index of Alteration (CIA) has the highest value of CIA in the bentonite-rich clay (74), while the CIA average value of sand-silt-clay is 59.2, and the loess deposits have 50.23 values. Thus, the CIA represents low to moderate chemical weathering. The K_2O/Al_2O_3 ratio of the studied sample shows that the original alkali feldspar is altered with low to moderate chemical weathering.

Furthermore, the Al_2O_3 - (CaO^*+Na_2O) - K_2O (A-CN-K) diagram classifies the differentiation of compositional variations associated with chemical weathering and/or source rock composition. In this diagram samples show weathering below the smectite-illite position, implying that chemical weathering is insignificant. It also shows that the studied samples have a moderate loss of Ca, Na, and K, as they tend to plot parallel to the A-CN. As a result, the positions of the samples in the A-CN-K diagram, as well as their CIA and PIA values, indicate that these sediments were formed from a rock source that experienced moderate chemical weathering. The Th/U value in the current instance, indicating minimal chemical weathering during the Plio-Pleistocene in Peshawar Basin.

Conclusion

The studied sections are the part of Plio-Pleistocene sedimentary archives in Peshawar Basin, Pakistan. Which is an interbedded succession of dominantly sand, silt, and clay rhythmites with interbedded conglomerates and overlain by repetitive loess. The sequence indicates basin formation in response to the Attock-Cherat uplift and maintains palaeoclimatic fluctuations and weathering trends during sedimentation. Bentonite-rich clay makes up the lowermost portion, while fine-grained siliciclastic deposits in floodplain environments make up the upper part with relatively high CIA values designates increasing trend in chemical weathering but still under cold-arid conditions. This unit is overlined by Lacustrine-Fluvial rhythmites of sand, silt, and scattered pebbles. The lack of red clay tops, mud cracks, and indications of extensive subaerial exposure support the idea that the Attock-Cherat Range's uplifting caused the deposition in a more stable, large lake. The Th/U vs. U plot shows that Lacustrine sediments are slightly more weathered than floodplain clay and loess. It is covered by conglomerates having dominancy of slaty clasts which support the fluvial influence. In the upper part presence of calcrete concretions and carbonate, horizons show that the sediment was deposited in arid settings with poor chemical weathering. Their arid position on the paleoclimatic proxy plots suggests dry paleoclimate during deposition, with aeolian transport processes dominating.

References

Abramowski, U., Bergau, A., Seebach, D., Zech, R., Glaser, B., Sosin, P., ... and Zech, W. (2006). Pleistocene glaciations of Central Asia: results from 10Be surface exposure ages of erratic boulders from the Pamir (Tajikistan), and the Alay–Turkestan range (Kyrgyzstan). *Quaternary Science Reviews*, *25*(9-10), 1080-1096.

Ali, K. A., & Anwar, J. (1969). Stratigraphic studies of the Nowshera reef complex, Nowshera Tehsil, West Pakistan. *Geological Bulletin of the University of Peshawar*, *4*, 33-43.

Bahlburg, H., and Dobrzinski, N. (2011). A review of the Chemical Index of Alteration (CIA) and its application to the study of Neoproterozoic glacial deposits and climate transitions. *Geological Society, London, Memoirs*, *36*(1), 81-92.

Bender, F., and Raza, H. A. (1995). Geology of Pakistan.

Bibi, M., Wagreich, M., Iqbal, S., and Jan, I. U. (2019). Regional sediment sources versus the Indus River system: The Plio-Pleistocene of the Peshawar basin (NW-Pakistan). *Sedimentary geology*, *389*, 26-41.

Bibi, M., Wagreich, M., Iqbal, S., Jan, I.U., 2019b. Regional sediment sources versus the Indus River system: the Plio-Pleistocene of the Peshawar basin (NWPakistan). Sedimentary Geol. 389, 26–41. https://doi.org/10.1016/j. sedgeo.2019.05.010).

Boggs Jr, S., and Boggs, S. (2009). *Petrology of sedimentary rocks*. Cambridge university press.

Buggle, B., Glaser, B., Hambach, U., Gerasimenko, N., and Marković, S. (2011). An evaluation of geochemical weathering indices in loess– paleosol studies. Quaternary International, 240(1), 12–21. http://doi. org/10.1016/j.quaint.2010.07.019

Burbank, D. W. (1983a). The chronology of intermontane-basin development in the northwestern Himalaya and the evolution of the Northwest Syntaxis. Earth and Planetary Science Letters, 64, 77–92. https://doi.org/10.1016/0012-821X(83)90054-7

Burbank, D. W., and Tahirkheli, R. K. (1985). The magnetostratigraphy, fission-track dating, and stratigraphic evolution of the Peshawar intermontane basin, northern Pakistan. *Geological Society of America Bulletin*, *96*(4), 539-552.

Calkin, P. E. (1974). Subglagial Geomorphology Surrounding the Ice-Free Valleys of Southern Victoria Land, Antarctica. *Journal of Glaciology*, *13*(69), 415-429.

Calkins, J. A., Offield, T. W., Abdullah, S.K.M., and Ali, S. T., 1974, Geology of the southern Himalaya in Hazara, Pakistan, and adjacent areas: United States Geological Survey Professional Paper 716-C, 27 p

Chevalier, M. L., Hilley, G., Tapponnier, P., Van Der Woerd, J., Liu-Zeng, J., Finkel, R. C., ... and Liu, X. (2011). Constraints on the late Quaternary glaciations in Tibet from cosmogenic exposure ages of moraine surfaces. *Quaternary Science Reviews*, *30*(5-6), 528-554.

Clift, P. D., Hodges, K. V., Heslop, D., Hannigan, R., Van Long, H., and Calves, G. (2008). Correlation of Himalayan exhumation rates and Asian monsoon intensity, Nat.Cornwell, K. (1998). Quaternary break-out flood sediments in the Peshawar basin of northern Pakistan. Geomorphology, 25(3–4), 225–248. https://doi.org/10.1016/S0169-555X(98)00061-0

Cornwell, K. (1998). Quaternary break-out flood sediments in the Peshawar basin of northern Pakistan. *Geomorphology*, *25*(3-4), 225-248.

Cotter, G. D. P. (1933). The geology of the part of the Attock district west of longitude 72 45 E. *Memoirs of the Geological Survey of India*, *55*(2), 63-161.

Coulson, A. L. (1938). General Report of the Geological Survey of India for the year 1937. *Rec. Geol. Suro. Ind*, *73*, 18-19.

DeCelles, P. G., Robinson, D. M., Quade, J., Ojha, T. P., Garzione, C. N., Copeland, P., and Upreti, B. N. (2001). Stratigraphy, structure, and tectonic evolution of the Himalayan fold-thrust belt in western Nepal. Tectonics, 20, 487–509. https://doi.org/10.1029/2000tc001226

Dickinson, W. R. (1970). Interpreting detrital modes of graywacke and arkose. *Journal of Sedimentary Research*, *40*(2), 695-707.

Dickinson, W. R., and Suczek, C. A. (1979). Plate tectonics and sandstone compositions. *Aapg Bulletin*, *63*(12), 2164-2182.

Ehlers, J., Gibbard, P. L., and Hughes, P. D. (2018). Chapter 4 – Quaternary glaciations and chronology past glacial environments (Second ed.) (pp. 77–101). Amsterdam, The Netherlands: Elsevier. https://doi.org/ 10.1016/B978-0-08-100524-8.00003-8

Fedo, C. M., Wayne Nesbitt, H., and Young, G. M. (1995). Unraveling the effects of potassium metasomatism in sedimentary rocks and paleosols, with implications for paleoweathering conditions and provenance. *Geology*, *23*(10), 921-924.

Fischer, G. (1999). *Use of Proxies in Paleoceanography: Examples from the South Atlantic; with 43 Tables*. Springer Science and Business Media.

Fischer, G., and Wefer, G. (Eds.) (2012). Use of proxies in paleoceanography: Examples from the South Atlantic (pp. 1–735). Berlin; New York: Springer Science and Business Media.

Fuchs, G. (1975). *Contributions to the geology of the North-Western Himalayas*. Geologische Bundesanstalt.

Gansser, A. (1964). Geology of the Himalayas (p. 289). New York: Interscience

Goldberg, K., & Humayun, M. (2010). The applicability of the Chemical Index of Alteration as a paleoclimatic indicator: An example from the Permian of the Paraná basin, Brazil. Palaeogeography, Palaeoclimatology, Palaeoecology, 293(1), 175–183. https://doi.org/10.1016/j.palaeo.2010.05.015

Goodbred, S. L. (2003). Response of the Ganges dispersal system to climate change: A source-to-sink view since the last interstade. Sedimentary Geology, 162, 83–104. https://doi.org/10.1016/S0037- 0738(03)00217-3

Graham, S. A., Ingersoll, R. V., and Dickinson, W. R. (1976). Common provenance for lithic grains in Carboniferous sandstones from Ouachita Mountains and Black Warrior Basin. *Journal of Sedimentary Research*, *46*(3), 620-632.

Hofmann, P., Ricken, W., Schwark, L., and Leythaeuser, D. (2001). Geochemical signature and related climatic-oceanographic processes for early Albian black shales: Site 417D, North Atlantic Ocean. *Cretaceous Research*, *22*(2), 243-257.

Hussain, A., Dipietro, J. A., & Pogue, K. R. (1998). Stratigraphy and structure of the Peshawar Basin, Pakistan. *Journal of Nepal Geological Society*, *18*, 25-35.

Ingersoll, R. V., and Suczek, C. A. (1979). Petrology and provenance of Neogene sand from Nicobar and Bengal fans, DSDP sites 211 and 218. *Journal of Sedimentary Research*, *49*(4), 1217-1228.

Ingersoll, R. V., Bullard, T. F., Ford, R. L., Grimm, J. P., Pickle, J. D., and Sares, S. W. (1984). The effect of grain size on detrital modes: a test of the Gazzi-Dickinson point-counting method. *Journal of Sedimentary Research*, *54*(1), 103-116.

Iqbal, S., Wagreich, M., Kuerschner, W. M., Gier, S., and Bibi, M. (2019). Hot-house climate during the Triassic/Jurassic transition: The evidence of climate change from the southern hemisphere (Salt Range, Pakistan). *Global and Planetary Change*, *172*, 15-32.

Kazmi, A. H., & Jan, M. Q. (1997). Geology and tectonic of Pakistan (pp. 130–141). Karachi: Graphic publication.

Klootwijk, C. T., Gee, J. S., Peirce, J. W., Smith, G. M., and McFadden, P. L. (1992). An early India-Asia contact: paleomagnetic constraints from Ninetyeast ridge, ODP Leg 121. *Geology*, *20*(5), 395-398.

Latif, M. A. (1970). Explanatory notes on the Geology of Southeastern Hazara, to accompany the revised Geological Map. *Wien Jb. Geol. BA, Sonderb*, *15*.

Malick, B. M. L., and Ishiga, H. (2016). Geochemical classification and determination of maturity source weathering in beach sands of eastern San'in Coast, Tango Peninsula, and Wakasa Bay, Japan. Earth Science Research, 5(1), 44. https://doi.org/10.5539/esr.v5n1p44

McLennan, S. M., Hemming, S., McDaniel, D. K., and Hanson, G. N. (1993). Geochemical approaches to sedimentation, provenance, and tectonics. *Special Papers-Geological Society of America*, 21-21.

Meissner, C. R., Master, J. M., Rashid, M. A., and Hussain, M. (1974). Geology of the Kohat Quadrangle, West Pakistan. *US Geological Survey, (IR)*, 1-75.

Menounos, B., Clague, J. J., Osborn, G., Davis, P. T., Ponce, F., Goehring, B., ... and Marr, R. (2013). Latest Pleistocene and Holocene glacier fluctuations in southernmost Tierra del Fuego, Argentina. *Quaternary Science Reviews*, *77*, 70-79.

Molloy, P. D., Talent, J. A., and Mawson, R. (1997). Late Devonian-Tournaisian conodonts from the eastern Khyber region, North-west Pakistan. *Rivista Italiana di Paleontologia e Stratigrafia*, *103*(2).

Molnar, P., and Tapponnier, P. (1975). Cenozoic Tectonics of Asia: Effects of a Continental Collision: Features of recent continental tectonics in Asia can be interpreted as results of the India-Eurasia collision. *Science*, *189*(4201), 419-426.

Nesbitt HW, Young GM (1982) Early Proterozoic climates and plate motions inferred from major element chemistry of lutites. Nature 299:715–717

Nesbitt HW, Young GM (1989) Formation and diagenesis of weathering profiles. J Geol 98:801–822

Nesbitt, H. W., and Young, G. M. (1984). Prediction of some weathering trends of plutonic and volcanic rocks based on thermodynamic and kinetic considerations. *Geochimica et cosmochimica acta*, *48*(7), 1523-1534.

Nesbitt, H. W., Young, G. M., McLennan, S. M., and Keays, R. R. (1996). Effects of chemical weathering and sorting on the petrogenesis of siliciclastic sediments, with implications for provenance studies. The Journal of Geology, 104(5), 525–542. https://doi.org/10.1086/629850

Nesbitt, I. I. W and Young GM (1982) Early Proterozoic climates and plate. *Nature*, *299*, 715-17.

Owen, L. A., Finkel, R. C., Caffee, M. W., and Gualtieri, L. (2002). Timing of multiple late Quaternary glaciations in the Hunza Valley, Karakoram Mountains, northern Pakistan: Defined by cosmogenic radionuclide dating of moraines. Geological Society of America Bulletin, 114(5), 593–604. https://doi.org/10.1130/0016-7606(2002)1142.0.CO;2

PakMet (2015). "Extremes of Peshawar". Pakistan Meteorological Department. Retrieved February 2, 2015.

Petterson, M. G., and Treloar, P. J. (2004). Volcanostratigraphy of arc volcanic sequences in the Kohistan arc, North Pakistan: volcanism within island arc, back-arc-basin, and intra-continental tectonic settings. *Journal of Volcanology and Geothermal Research*, *130*(1-2), 147-178.

Pivnik, D. A., and Johnson, G. D. (1995). Depositional response to Pliocene–Pleistocene foreland partitioning in northwest Pakistan. *Geological Society of America Bulletin*, *107*(8), 895-922.

Selvaraj, K., and Chen, C. T. A. (2006). Moderate chemical weathering of subtropical Taiwan: constraints from solid-phase geochemistry of sediments and sedimentary rocks. *The Journal of Geology*, *114*(1), 101-116.

Selvaraj, K., Mohan, V. R., and Szefer, P. (2004). Evaluation of metal contamination in coastal sediments of the Bay of Bengal, India: geochemical and statistical approaches. *Marine pollution bulletin*, *49*(3), 174-185.

Singh, A. K., Parkash, B., Mohindra, R., Thomas, J. V., and Singhvi, A. K. (2001). Quaternary alluvial fan sedimentation in the Dehradun Valley Piggyback basin, NW Himalaya: Tectonic and palaeoclimatic implications. Basin Research, 13, 449–471. https://doi.org/10.1046/j.0950- 091x.2001.00160.x

Stübner, K., Grin, E., Hidy, A. J., Schaller, M., Gold, R. D., Ratschbacher, L., and Ehlers, T. (2017). Middle and Late Pleistocene glaciations in the southwestern Pamir and their effects on topography. *Earth and Planetary Science Letters*, *466*, 181-194.

Suttner, L. J., and Dutta, P. K. (1986). Alluvial sandstone composition and paleoclimate; I, Framework mineralogy. *Journal of Sedimentary Research*, *56*(3), 329-345.

Tahirkheli, R. A. K. (1970). The geology of the Attock-Cherat Range. Geological Bulletin University of Peshawar, 5

Taylor, S. R., and McLennan, S. M. (1985). The continental crust: its composition and evolution.

Teichert, C., and Stauffer, K. W. (1965). Paleozoic reef in Pakistan. *Science*, *150*(3701), 1287-1288.

Yan, D., Chen, D., Wang, Q., and Wang, J. (2010). Large-scale climatic fluctuations in the latest Ordovician on the Yangtze block, south China. *Geology*, *38*(7), 599-602.

Yeats, R. S., and Hussain, A. (1987). Timing of structural events in the Himalayan foothills of northwestern Pakistan. *Geological society of America bulletin*, *99*(2), 161-176.

Yin, A., and Harrison, T. M. (2000). Geologic evolution of the Himalayan-Tibetan orogen. *Annual review of earth and planetary sciences*, *28*(1), 211-280.